DM

A Strategy to Increase the Production of Extracellular Polymeric Substances

Industrial valorization of *Cyanocohniella Calida* and its application in microplastic removal

MASTER DISSERTATION

Ricardo André Ferreira Gomes
MASTER IN APPLIED BIOCHEMISTRY

UNIVERSIDADE da MADEIRA
A Nossa Universidade
www.uma.pt

September | 2022

A Strategy to Increase the Production of Extracellular Polymeric Substances

Industrial valorization of *Cyanocohniella Calida* and its application in microplastic removal

MASTER DISSERTATION

Ricardo André Ferreira Gomes
MASTER IN APPLIED BIOCHEMISTRY

ORIENTATION
Nereida Maria Abano Cordeiro

Acknowledgements

I would like to thank everyone who helped with my master's thesis in any manner, whether on a professional, inspirational or personal level, making its execution possible.

To my supervisor, Professor Doctor Nereida Cordeiro, for her unwavering support, scientific guidance, encouragement, patience, and constructive criticism, and for making available the necessary materials for the execution of this thesis.

I want to express my gratitude to the entire working group at the LB3- Laboratory of Bioanalysis, Biomaterials & Biotechnology, the University of Madeira, for sharing their knowledge with me, for all the help, advice, and for giving the resources needed to complete this study.

To my closer friends, I express my gratitude for their unconditional friendship, support, and patience throughout these years.

Finally, I express my profound gratitude to my parents and my girlfriend, for providing me with unfailing support and continuous encouragement throughout the last couple of years of study and through the process of researching and writing this thesis. This accomplishment would not have been possible without them. Thank you.

Abstract

Microplastics (MPs) are present in all types of water, proving to be a risk to both environment and human health. These contaminants also may affect the algal industry, leading to significant economic losses. Therefore, creating sustainable and efficient removal methods is essential. Microbial exopolysaccharides (EPS) have demonstrated an ability to remove water contaminants. Their network-like appearance structure encourages particle agglomeration. This work's goals are: *(i)* to propose an industrial operation strategy to enhance EPS *Cyanocohniella calida* production; *(ii)* evaluate the cyanobacteria EPS behaviour in the presence of MPs; *(iii)* and verify the EPS bioflocculant potential, in view of its industrial valorisation. The response surface methodology (RSM) was employed to find better conditions for EPS production. The developed model evaluated the number of days (0-7), nitrogen concentration (2.5-10 g/dm^3), phosphorous concentration (0.5-2 g/dm^3), and ratio (1:1-1:14) (cyanobacteria/culture medium). The best conditions were 7 days of production, with 10 g/dm^3 of nitrogen, 0.98 g/dm^3 of phosphorus, and a biomass/culture medium ratio of 1/6.87, for an EPS production efficiency of 113 mg/dm^3. *C. cf. calida* was placed in MPs-contaminated water at low (0.05 mg/dm^3) and high (5 mg/dm^3) concentrations, under static and aerated conditions, and in two distinct growth stages (exponential and stationary). Higher EPS production (231 mg/dm^3) was achieved in the exponential growth stage under aerated conditions and when exposed to environmental concentrations of MPs (0.05 mg/dm^3). To determine the bioflocculant activity of the produced EPS in water highly contaminated with MPs (2 g/dm^3), the type of cation present, its concentration, pH, salinity, and EPS/MPs ratio were examined. The highest bioflocculation rates (82%) were obtained in freshwater with an EPS/MPs ratio of 1/5, 0.05% (w/w) Fe^{3+}, pH 3.5 ± 0.1, a temperature of 25 ± 2 °C, and an EPS solution with a concentration of 400 mg/dm^3. Thus, *C. cf. calida* demonstrates *(i)* high potential as an EPS producer; *(ii)* EPS production stimulation in the presence of MPs-contaminated water; and *(iii)* the EPS produced is an efficient, suitable, and environmentally friendly solution to remove MPS from contaminated water for use in the algal industry.

Keywords:

Cyanobacteria; *Cyanocohniella calida*; exopolysaccharides; microalgae; microplastics; bioflocculation.

Resumo

Os microplásticos (MPs) estão presentes em todos os tipos de água demonstrando ser um risco para o ambiente bem como para a saúde humana. Estes contaminantes também podem afetar a indústria de algas, levando a prejuízos económicos avultados. Consequentemente, é importante criar métodos para uma remoção sustentável e eficiente. Os exopolissacáridos (EPS) de origem microbiana têm demonstrado capacidade para remover contaminantes presentes na água graças à sua estrutura em rede, que permite e facilita a aglomeração de partículas. Os objetivos do presente trabalho são: *(i)* propor uma estratégia de operação industrial para melhorar a produção de EPS da *Cyanocohniella calida*; *(ii)* avaliar o efeito da presença de MPs nos EPS da cianobactéria; *(iii)* e verificar o potencial biofloculante dos EPS, tendo em vista a sua valorização industrial. A metodologia de resposta de superfície (RSM-*Response Surface Methodology*) foi utilizada para encontrar as melhores condições para a produção dos EPS. O modelo desenvolvido avaliou o número de dias (0-7), concentração de azoto (2,5-10 g/dm^3), concentração de fósforo (0,5-2 g/dm^3) e a razão cianobactérias/meio de cultura (1:1-1:14). As melhores condições demonstraram ser 7 dias de produção, com 10 g/dm^3 de azoto, 0,98 g/dm^3 de fósforo, e uma razão de biomassa/meio de cultura de 1/6,87 para uma eficiência de produção de EPS de 113 mg/dm^3. A *C. cf. calida* foi exposta a água contaminada com MPs em concentrações baixas (0,05 mg/dm^3) e altas (5 mg/dm^3), sob condições estáticas e de arejamento, e em duas fases distintas de crescimento (exponencial e estacionária). A maior produção de EPS (231 mg/dm^3) foi alcançada na fase de crescimento exponencial sob condições de arejamento e quando expostos a concentrações ambientais de MPs (0.05 mg/dm^3). De modo a conhecer a atividade biofloculante dos EPS produzidos foram usadas águas altamente contaminadas com MPs (2 g/dm^3), o tipo de catião presente e a sua concentração, o pH, a salinidade, e o rácio EPS/MPs foram estudados. As maiores taxas de biofloculação (82%) foram obtidas para um rácio EPS/MPs de 1/5, contendo 0.05% (*p/p*) Fe^{3+}, pH 3,5 ± 0,1, temperatura de 25 ± 2 °C, e uma solução de EPS com uma concentração de 400 mg/dm^3. Desta forma, a *C. cf. calida* demonstrou: *(i)* elevado potencial como produtora de EPS; *(ii)* produção de EPS estimulada na presença de águas contaminadas por MPs; e *(iii)* os EPS produzidos são uma solução eficiente, adequada e amiga do ambiente para remover MPs de águas contaminadas a usar na indústria de algas.

Palavras-chave:

Cianobactérias; *Cyanocohniella calida;* exopolissacáridos; microalgas; microplásticos; biofloculação.

Table of Contents

Chapter 3- Results and discussion

List of Figures

List of Tables

Chapter 1

Introduction

1.1 Cyanobacteria and exopolysaccharides

Cyanobacteria and microalgae are important trophic chain components within marine and aquatic photosynthetic organisms. Microalgae are eukaryotic unicellular organisms, including those from Chlorophyceae, Eustigmatophyceae and Bacillariophyceae classes; however, cyanobacteria are prokaryotic photosynthetic organisms [1]. Cyanobacteria are key and pioneer organisms in soil crusts, capable of providing the nutrient source for other living heterotrophic organisms. These can provide nutrients through nitrogen fixation, carbon sequestration and the release of nutrient-rich exopolysaccharides [2,3]. Their photoautotrophic nature, capacity to fix atmospheric N_2, low light demand, ubiquity, quick generation time, self-sufficiency in growth and maintenance, and adaptability to survive in extremely polluted environments show that cyanobacteria have certain benefits over other microorganisms [2,4]. Ponds, lakes, water streams, rivers, and wetlands all have them. They can readily endure harsh settings, including hot springs, high salty water, subfreezing temperatures, and deserts. Cyanobacteria can thrive in a temperature range of 45 – 70°C and environments with a pH lower than 4 - 5, with an ideal range of 7.5 – 10°C [3].

Cyanocohniella is a genus of cyanobacteria in the family of *Aphanizomenonaceae* that have a hypervariable morphology and one of the most complex life cycles among all Cyanobacteria [5]. The population of *Cyanocohniella. calida (C. calida)* has a polymorphic life cycle. Hormogonia and immature filaments have: isodiametric to cylindrical cells that are 1.5 mm wide, neither constricted or just slightly constricted at the cross walls; intercalary cells that are 1.5 – 2.5 mm long; and apical cells that are 1.5 – 2.5 mm long and longer than broad. Despite appearing to be a thermal species, *C. cf. calida* is really eurythermal. The thermal tolerance offers a competitive advantage among taxa that overgrow in unfavourable thermal conditions [5].

Cyanobacteria are involved in producing secondary metabolites, such as exopolysaccharides (EPS), with great industrial importance and, therefore, a potential source of EPS. These EPS play prominent roles on cell protection and biofilms/colonies formation, and have distinct features compared to other bacterial EPS [5,6]. However, various adjustments can be made to the production process to make it more efficient and achieve economic viability. Depending on the strain, changes in cultivation/growth circumstances can affect the amount and composition of EPS [6,7]. It is important to stream any variables affecting the amount released into the culture medium. These variables mostly have an operational aspect, and cyanobacteria cells can assimilate them as stressors. Indeed, it appears that the main factors to consider in increasing EPS production yields are the availability of macro and micronutrients (and any condition of deficiency linked with it), salinity, temperature, gases exchange or

irradiance [8]. The metabolic pathways for EPS build-up have yet to be fully elucidated. Therefore, it´s hard to establish the appropriate parameters that affect EPS production for a specific strain. As a result, it takes multiple tests with one or more factors for each strain to determine if there is an EPS production improvement [8].

Due to its quick production time and straightforward isolating process, microbial EPS, particularly those of bacterial origin, are gaining increasing attention. It is possible to produce these polymers without using chemicals that harm the environment [6]. Cyanobacteria can also provide a sustainable platform for manufacturing polymers due to their low nutritional needs. Furthermore, unlike heterotrophic bacteria cultivation, their photosynthetic metabolism permits large-scale outdoor cultivation with lower energy costs [6].

EPS are macromolecules or biosynthetic polymers secreted by developing microorganisms in a natural or artificial environment. These complex molecules with high molecular weight vary in composition based on the type of microbe and environment [9]. EPS are primarily composed of heteropolysaccharides, which comprise proteins, polysaccharides, nucleic acid, and humic acid. This makes EPS a biopolymer and plays a central role in microbial aggregation and biofilm formation [10,11]. EPS present a distinctive set of industrially desirable features, including strong anionic nature, sulphate groups, a wide variety of possible structural conformations and amphiphilic behaviour [6,7].

EPS can present itself either wholly expelled into the surrounding medium or more or less securely linked to the cells, depending on the microbe. The "free" polymers (Figure 1 A) are known as mucilage or released exopolysaccharides (RPS), while the bound polymers (Figure 1 B) are often called bound polysaccharides or capsular exopolysaccharides (CPS) [12,13].

It is generally accepted that, in the particular case of *C. cf. calida*, most exocellular polysaccharides are composed of RPS, with only a minor fraction identified as CPS [13].

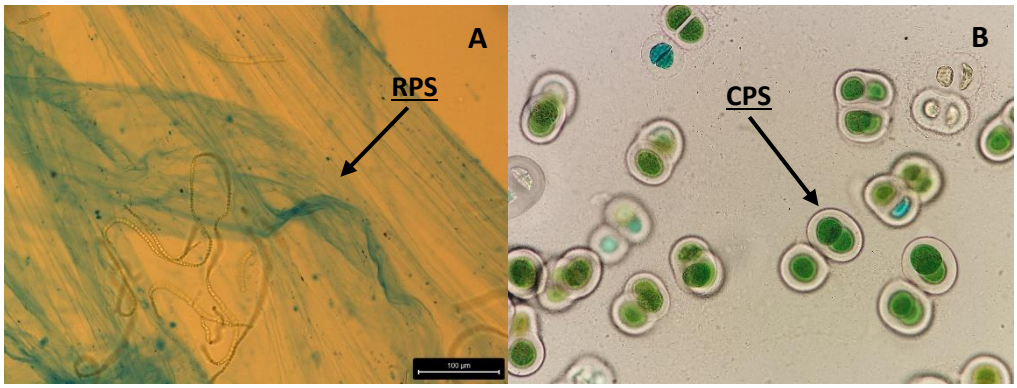

Figure 1 Pictures of RPS-producing cyanobacteria (*Cyanocohniella cf. calida*) stained with Alcian Blue (A); CPS-producing cyanobacteria (*Gloeocapsa sp.*) (B).

RPS exhibit a wide range of physicochemical characteristics, including solubility, viscosity, gelling capacity, chain length (degree of polymerisation), linkage types and patterns, giving them the adaptability to be employed in significant commercial sectors like food, medicines, biomedicine, electronics and bioremediation [6]. Cyanobacteria RPS are more complex than the RPS produced by other microorganisms due to the high diversity of monosaccharides building blocks and consequent variety of linkages, demonstrating physical-chemical characteristics appropriate for the industry as gums, bioflocculants, soil conditioners, biolubrificants, and biosorbents [6].

The RPS matrix has a crucial role in microbial aggregates and sludge characteristics, such as their capacity for flocculation, settleability, surface characteristics, dewaterability and adsorption [10]. RPS presents itself as a sustainable alternative for water treatment, specifically for removing particles like MPs, due to its impressive flocculating capacity [14,15].

The IUPAC (International Union of Pure and Applied Chemistry) defines flocculation as a contact and adhesion process in which the dispersion of particles results in the formation of large-size clusters. Bioflocculation is used when this process occurs spontaneously and is mediated by microorganisms and their products. Due to the dangers associated with synthetic inorganic and organic flocculants, microbial flocculants are receiving more attention [7, 16]. The efficiency of bioflocculation depends on several coculturing factors, including pH, temperature, Ca^{2+} concentration, salt content, and type of cyanobacteria product used [12,16,17]. There have been reports of some freshwater cyanobacteria with the ability to produce RPS with flocculating activity [16].

Due to its cost, low energy need, and non-toxicity, bioflocculation has attracted interest as an alternative for wastewater treatment and MPs removal [7]. Over the last 30 years, several physical, chemical, and biological removal procedures, including flotation, precipitation, oxidation, solvent extraction, evaporation, carbon adsorption, ion exchange, membrane filtration, electrochemistry, biodegradation, and phytoremediation, have been documented [19]. However, the use of cyanobacteria products in flocculation processes is yet to be truly explored. High flocculation efficiencies have been seen in wastewater treated using cyanobacterial cultures, mainly when using filamentous cyanobacteria [18].

1.2 Microplastics

For a long time, numerous initiatives have been made to reduce environmental pollution by risky substances, including toxic elements and particles, that can have adverse effects [4].

The most prevalent contaminants present in marine and urban hydro systems today are microplastics (MPs) [20]. MPs can absorb various persistent organic pollutants from the water around them, which could enrich these pollutants [20]. They have been found in all water forms, from wastewater to drinking water, resultant from both commercial products that have microplastics or the breakdown of larger plastics, posing a threat to both the environment and human health. Urban effluents from wastewater treatment plants are suspected of containing MPs, demonstrating that conventional treatment processes of these urban effluents cannot wholly remove MPs [20]. Therefore, it is crucial to develop and improve removal techniques [21,22].

Cyanobacteria products can accumulate or degrade a wide range of environmental contaminants, including pesticides, crude oil, naphthalene, phenanthrene, phenol, heavy metals, and xenobiotics [2]. Their particle accumulation ability is of particular interest and could present itself as an alternative for MPs removal processes. Studies have demonstrated the potential of biological materials produced by bacteria, fungi, and algae in removing pollutants, having the benefits of being more affordable and readily available [2,4].

1.3 Response Surface Methodology

In order to account for the component's interacting effects and optimise the result, recent innovations have seen the introduction of statistical approaches, like response surface methodology (RSM), in replacement of the conventional "one factor at a time" (OFAT) approach [23,24]. Because so many experiments are required, the traditional OFAT approach is time-consuming and cannot explain how different factors interact. This makes it challenging to determine these factors' true optimum values [24]. In contrast, using a statistical optimisation design saves production costs by avoiding the need for numerous runs. To build production models, the RSM combines statistical and mathematical methods, analysing the impact of multiple independent factors to determine the optimal value of each variable to maximise production. This plays a significant role in the conception, creation, and formulation of new goods, as well as the advancement of existing product designs [4,24].

The RSM was developed in 1951 by Box and Wilson. Their method involved first utilising the Design of experiment (DoE) to determine which factors significantly affected the measured variations of a response and to build a low-order polynomial equation to forecast the response [25]. The majority of RSM's real-world applications will provide several responses. The engineer or scientist controls the input variables, also known as independent variables, at least for the duration of a test or experiment [26].

Even though the resultant quantitative connection is empirical, there is a significant benefit in the pace of testing and the high possibility that a useful model will be developed to distinguish underperforming methods from effective ones and optimise industrial production processes [25].

1.4 Aim of the study

In light of EPS potential industrial value, the work's goal can be described into three steps: *(i)* to provide an industrial operation strategy to increase RPS production, or in this case, *C. cf. calida* -based RPS, *(ii)* to evaluate the cyanobacteria behaviour in the presence of MPs, analysing the impact that the presence of MPs has on both, RPS production and cyanobacteria biomass; and *(iii)* verify the RPS bioflocculant potential, as well as their sticky character, capable of creating aggregates by tying together small particles, like MPs - in view of its industrial valorisation.

The findings may allow further investigation of *Cyanocohniella cf. calida's* capacity to manufacture RPS use in biotechnological and industrial domains, as well as presenting itself as a possible method for wastewater treatment, more specifically as a method to remove MPs.

Another interesting step worth exploring in the future, which may present a possible improvement in RPS production at an industrial level, is creating a zero-waste value chain, which includes recycling waste biomass.

Chapter 2

Material and Methods

2.1 Cyanobacteria and growth conditions

Cyanocohniella cf. calida (BEA 0786B) was found in hypersaline environments in Spain, more precisely at Álava in the Añana Saltworks and provided by Spanish Microalgae Bank. *C. cf. calida* grew in Spirulina medium, under an irradiance of 40 µmol.photons.m^{-2}.s^{-1} (HOBO® Pendant® MX Temp MX2202) with a 14/10 h (Light (L)/Dark (D)) photoperiod (Aralab CP500 growth chamber) at 22 ± 1°C until reaching the stationary phase (1.08 Optical Density (OD)).

To study the cyanobacteria behaviour in the presence of Polystyrene Microplastics (PS-MPs), *C. cf. calida* cultures were subjected to PS-MPs -contaminated waters at low (0.05 mg/dm^3) and high (5 mg/dm^3) concentrations under various aeration settings (static culture and under aeration flux) during a seven-day trial period. (0.75 OD) All the experiments were performed with at least three replicates.

2.2 Microplastics

The PS-MPs used came from commercial yellow polystyrene (PS) (UV-Granulate, Magical Pyramid Bruecher&Partner KG, Frechen, Germany) and were ground using a milling machine (230 V, 50 Hz, 120 W) until obtained a fraction lower than 100 µm. The particle size was confirmed using a sieve with a fraction of 100 µm. After grinding and fractionation, PS-MPs were washed with *n*-hexane to remove possible surface contaminants. Then, PS-MPs were filtered using a G4 filter crucible, oven-dried overnight at 60 °C and kept in a desiccator until further use. Two culture medium stock solutions of PS- PS-MPs were prepared in the presence of Tween 20 (0.1%; v/v) (to guarantee the homogenisation of the solutions): low environmental concentration (0.05 mg/dm^3) and high concentration (5 mg/dm^3).

2.3 Experimental design

Experimental design 1: The ratio (cyanobacterial biomass/culture medium), number of days of growth, nitrogen concentration, and phosphorus concentration were examined separately as the four variables with the most significant influence on the development and abundance of cyanobacteria. The one factor-at-a-time (OFAT) outcome made it possible to determine each factor's range for the RSM application: ratio (1:1-1:14), days (1-7), phosphorous concentration (0.5-2 g/dm^3), nitrogen concentration (2.5-10 g/dm^3). The obtained *C. cf. calida* -based RPS values were determined for each model experiment using the Alcian Blue quantification technique [26]. The RPS solution was stained in a 1:3 ratio (1 Alcian Blue to 3 RPS solution), and a spectrophotometer was used to measure the optical density at 610 nm. Using

linear regression, the spectrophotometry results were examined. Linearity was achieved by plotting eight different concentrations of *C. cf. calida* -based RPS (0.05, 0.1, 0.25, 0.3, 0.35, 0.4, 0.45, 0.5 mg/dm^3), including a blank. The equation obtained was y = 99.9 x + 18, with a correlation coefficient (R^2) of approximately 0.95 (Figure A1).

Experimental design 2: The effect of PS- PS-MPs in the *C. cf. calida* growth medium was evaluated. An initial selected biomass was fixed as 16g to ensure the homogeneity of culture. Cellular growth was monitored throughout the experiment. 10 mL of culture was taken under aseptic conditions, centrifuged at 4427 *g* for 10 min (HERLME Z360 Centrifuge), and then oven-dried at 40°C until constant weight. The existence of RPS and changes in cell morphology were examined through optical microscopy after Alcian Blue staining (methodology described in section 2.6.1). Viscosity was monitored to evaluate the effect of PS- PS-MPs on the RPS production by *C. cf. calida* (methodology described in section 2.6.2).

Experimental design 3: The bioflocculant activity, by RPS, of PS-MPs contained in contaminated waters was evaluated. Different parameters were studied: the cation type (Fe^{3+}, Ca^{2+}, Mg^{2+} and K^{+} (0.448mM)), Fe^{3+} concentration (0.03-0.95%), pH (3-7), salinity (0, 15 and 37‰), RPS/MPs ratio (4, 40, 400 and 500 mg/dm^3), and resting time (30, 60, 120 min) under controlled temperature conditions (25 ± 2 °C).

2.4 Response Surface Methodology modelling

Design Expert software (Design-Expert. 13. Stat-Ease, 2021.) was used to *(i)* generate a three-level, four-factor fractional factorial experimental design approach with a total of 78 tests, which was performed during the experimental study; *(ii)* fit the experimental results with the model second order polynomial; (*iii*) analyse the model validity, as well as the significance of the factors, and (*iv*) optimise the method for the best outcome.

To check the model's validity, several statistical analyses are taken into account: *1*- Residuals analysis is the principal tool used to diagnose model adequacy, as well as the analysis of variance (ANOVA). Residuals are the difference between any data point and the regression line [26]; *2*- Analysis of the lack of fit, which is the difference between the model prediction values and the average of the replicated runs carried out under the same experimental conditions; *3*- Analysis of the *F*-value and *p*-value, provided by the ANOVA test. With these tests, it is possible to verify the impact of each factor on the product outcome.

2.5 RPS isolation and purification

The supernatants obtained by centrifugation of the biomass were put through an ultrafiltration system to purify the expelled polymeric substances. Briefly, using an ultrafiltration unit (Vivaflow 50R, Sartorius), the supernatant is compelled through a 10 kDa cut-off membrane. Water and low-molecular-weight solutes pass through the membrane to the permeate side, while suspended particles and high-molecular-weight solutes stay on the retentate side. By performing 12 consecutive cycles of concentration and dilution (2.5x) with bidistilled water to obtain a constant conductivity (2.7 S/cm^3; Consort C5020), the removal of inorganic contaminants and low molecular weight compounds was ensured. The measurements were performed with at least three replicates.

2.6 Characterisation methods

2.6.1 Optical microscopy

RPS and the changes in cell morphology were examined using a *Leica DM2700P microscope coupled with a Leica DFC450 C digital camera* after Alcian Blue staining [26]. The Alcian blue staining technique involves mixing 50 mL of each sample with 50 mL of dye in an eppendorf. The mixture was then homogenised and allowed to stand for 30 min. An aliquot was transferred to a slide, and the observations were carried out.

2.6.2 Viscosity

As an indicator of RPS production, medium viscosity was monitored using a programmable Rheometer (Brookfield DV-III Ultra Programmable Rheometer) with a spindle 02 at 100 rpm. For the bioflocculation experiment, viscosity monitoring occurred under different temperature conditions (15-40°C). The measurements were performed with at least three replicates.

2.6.3 Scanning electron microscopy (SEM)

The RPS solution was fixed using 2.5% (w/v) glutaraldehyde in 0.1 M sodium phosphate buffer at pH 7.2 and kept at 4°C overnight. The samples were then rinsed twice with 0.1 M sodium phosphate buffer at pH 7.2. These were then serially dehydrated with ethanol (30, 50, 70, 90, and 100%, v/v, ethanol/water) before freeze-drying. After that, samples were kept dry until analysis in a desiccator. A Hitachi (Tokyo, Japan) HR-FESEM SU-70 microscope operating at 4.0 kV in field emission mode was used to capture the SEM micrographs. To do so, the samples were coated with carbon on a steel plate using an EMITECH K950X Turbo Evaporator.

2.6.4 Fourier-transform infrared spectroscopy (FTIR)

A PerkinElmer infrared spectrophotometer, Spectrum Two was used to create the FTIR spectra of RPS. Before the analysis, the materials were homogenised with KBr after being dried at 40 °C for 48 hours. The spectra were obtained between 4000 and 700 cm^{-1}, with a resolution of 1 cm^{-1} and after 32 accumulation scans.

2.6.5 Zeta potential

The surface charge of the *C. cf. calida* -based RPS was measured using the Zeta potential. Using a Zetasizer Nano ZSP (Malvern), the zeta potential was measured in Mili-Q water at 25 °C (pH 7). The measurements were performed with at least three replicates.

2.6.6 Bioflocculant activity

To study the bioflocculant activity of *C. cf. calida* -based RPS to remove PS-MPs from contaminated waters, the following parameters were studied: cation type (Fe^{3+}, Ca^{2+}, Mg^{2+} and K^{+} (0.448 mM)), Fe^{3+} concentration (0.03-0.95%), pH (3-7), salinity (0, 15, 37‰), RPS/PS-MPs ratio (4, 40, 400 and 500 mg/dm^3), and resting time (30, 60, 120 min).

Under tightly controlled temperature conditions (25 ± 2 °C), 0.2 ml of the RPS solution and 0.5 ml of the cation (various concentrations) were combined. 9.3 ml of the PS-MPs solution and 0.5 ml of the cation were placed in a tube and stirred on a stirring plate for 5 minutes at 700 rpm. The RPS solution was added, and the mixture was stirred once more for 30 minutes at 100 rpm. Subsequently, the samples had time to settle. 1 ml from the middle layer supernatant was taken, and a UV-6300PC Double Beam Spectrophotometer was used to measure the absorbance at 750 nm (OD_{750nm}) in a quartz cell. The bioflocculation activity was quantified by the bioflocculation rate (%) (Eq. 1). The measurements were performed with at least three replicates.

$$Bioflocculation\ activity = \left(\frac{OD750b - OD750s}{OD750s}\right) * 100 \qquad \text{Eq. 1}$$

where OD_{750s} and OD_{750b} represent the absorbance of the solution and blank, respectively.

2.6.7 Statistical Treatment

Statistical analysis of all obtained data was carried out using Design Expert (Design-Expert. 13. Stat-Ease, 2021.) and GraphPad (GraphPad: Prism. 9. Dotmatics, 2020). The

differences in cyanobacteria growth and RPS production when exposed to PS-MPs, and the bioflocculant activity of RPS to remove PS-MPs from contaminated waters, were assessed by one-way analyses of variance (ANOVA). The results were considered statistically significant if the *p*-value was lower than 0.05.

Chapter 3

Results and discussion

3.1 Industrial operation strategy to enhance RPS production

Response surface methodology (RSM) provided by Design of Experiment are tools that help industrial and non-industrial processes to perform at their best. RSM creates accurate maps using mathematical models. This methodology makes it easier to combine all solutions using complex optimisation techniques and identifying sweet spots where it can meet all the requirements at the lowest possible cost [31,32].

Given the first objective of this work - to provide an industrial operation strategy to increase RPS production - the RSM was used to optimise the production of RPS by checking essential factors for growth.

3.1.1 RSM applicability

Setting the levels for each research variable was the first step in applying the RSM. Several factors, such as ratio (cyanobacterial biomass(g)/culture medium(mL)), days, nitrogen, and phosphorous concentration, were tested using the one factor-at-a-time (OFAT) methodology. To assess the impact on RPS synthesis when cyanobacteria have a higher or lower nutrient availability, various ratios (cyanobacterial biomass/culture medium) were analysed. Cyanobacteria are particularly well known for being diazotrophs (they develop at the expense of nitrogen (N)) and for utilising phosphorus (P) as a critical ingredient for storage and the exchange of energy and information in the cell [33,34]. A study of RPS production ranging the concentrations of these nutrients was conducted as a result of these characteristics.

Despite providing valuable information regarding the impact of each factor on RPS production, the OFAT methodology ignores the potential for factor interaction [29,35,36,37] .Thus, a three-level, four-factor fractional factorial experimental design approach was used to assess the impact of various parameters on RPS production. Table 1 displays the RPS production variables: ratio (biomass(g)/culture medium (mL)), days (units), phosphorous concentration (g/dm^3) and nitrogen concentration (g/dm^3), associated with the respective coded variable (A, B, C, D). Since each variable has measurable properties and is either finite or countably infinite, all the variables are discrete [29].

Table 1 Process variables and respective coded and experimental levels for optimising RPS production. -1: factor at low level; 0: factor at medium level; +1: factor at high level

Variables	Coded variables	Units	Type of variable	Real values of coded levels		
				-1	0	1
Ratio (biomass/culture medium)	A	g/mL	Discrete	1:1	1:7	1:14
Days	B	units	Discrete	1	4	7
Phosphorus concentration	C	g/dm^3	Discrete	0.5	1.25	2
Nitrogen concentration	D	g/dm^3	Discrete	2.5	6.25	10

A second-order polynomial (model) was automatically applied to fit the experimental results (Eq. 1) and describe the interactions between the process variables (A, B, C and D) and the response variable Y (RPS concentration):

$$Y=X_0 + X_1 A + X_2 B + X_3 C + X_4 D + X_{12} AB + X_{13} AC + X_{14} AD + X_{23} BC + X_{24} BD + X_{34} CD + X_{11} AA + X_{22} BB + X_{33} CC + X_{44} DD \quad (Eq.\ 1)$$

The equation is composed of the predicted response Y, the model constant X_0, the linear coefficients X_1, X_2, X_3 and X_4, the cross-product coefficient X_{12}, X_{13}, X_{14}, X_{23}, X_{24} and b_{34} and the quadratic coefficients X_{11}, X_{22}, X_{33}, X_{44} [27].

RSM generated a total of 78 tests (Table A1), which were performed experimentally. The 78 tests consist of 26 different RPS production conditions in triplicate. A quadratic polynomial regression equation based on the coded parameters (*Eq. 1*) that links the independent factors to the response (y; RPS yield) was fitted to the experimental RPS concentration values that were measured:

$$Y=147.43 - 41.31 A + 14.92 B + 0.7880 C + 11.85 D + 23.6 AB - 8.01 AC + 9.26 AD - 2.23 BC - 0.4639 BD - 1.91 CD + 37.87 A^2 - 4.29 B^2 - 11.57 CC - 4.47 D^2 \quad (Eq.\ 2)$$

It's possible to compare the experimental values obtained by the experimental study (Table A1) to those predicted by the model (*Eq. 2*). The differences between the predicted and experimental data are relatively small - the experimental RPS concentration ranged from 60.87 to 267 mg/dm^3. In comparison, the predicted RPS concentration ranged from 60 to 227 mg/dm^3, depending on the combination of process parameters.

Residuals (Figure 2), lack-of-fit (Table A2) and ANOVA (Table A2) analysis were the major statistical factors considered while evaluating the applicability of the model. As shown by Figure 2 (A1), the Residual vs Predicted values have a uniform distribution, and the absence of outliers indicates no overt signs of normality. Also, the coefficient of determination (R^2 = 0.9417) obtained from the Predicted *vs* experimental values (Figure 2 (B1)) corroborates the *Eq. 1* suitability to model the RPS production variables.

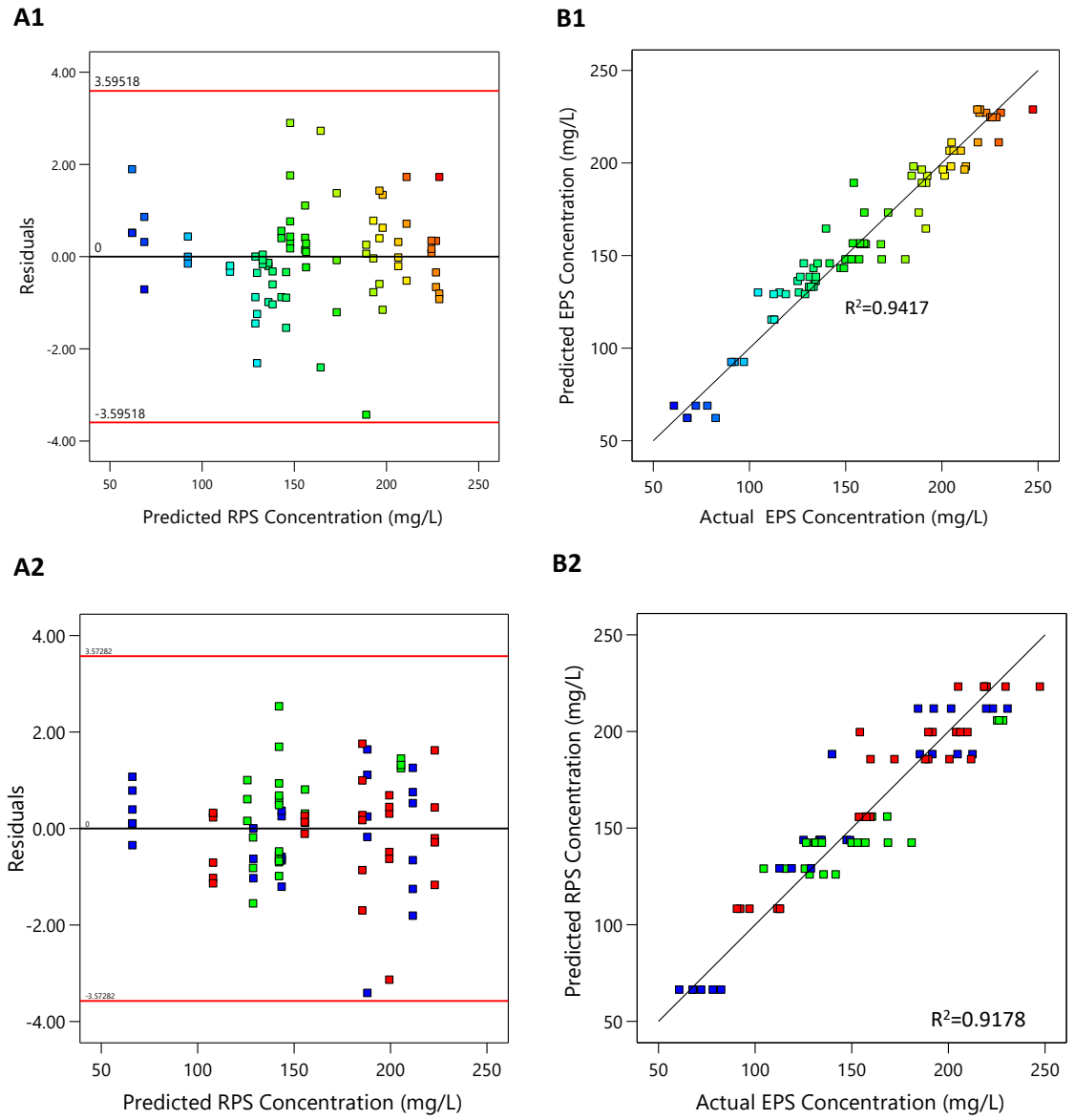

Figure 2 Model diagnostic plots for the general (1; A1 and B1) reduced (2; A2, B2) model: Residual plot for predicted RPS concentration **(A)**, Predicted RPS concentration *vs* experimental **(B).**

The analysis of variance (ANOVA) with the model's sum of squares of 1.59 x 10^5, 14 degrees of freedom, and mean square of 11361,83 was a crucial input for the model's evaluation. The *p*-value less than 0.05 and the F-value of 40.06 (greater than the critical value $F_{(0.05, 14, 63)}$ = 1.835) led to the conclusion that the model is applicable. Also, the analysis of the lack of fit (Table A2) with a *p*-value of 0.0561 (non-significant) approved the adequacy fitting of the model. On the other hand, the coefficient of determination analysis (Table A3) didn't reveal a significant discrepancy between the predicted R^2 (0.9092) and the adjusted R^2 (0.9285). This finding suggests that the factors in the model are statistically significant [25].

However, to verify the significance of the model terms and simplify the empirical model generated, ANOVA analysis was performed (Table A2) [39]. A *p*-value less than 0.05 indicates the significance of the model terms; thus, the model terms A, B, D, AB, AC, AD, A^2 and C^2 are significant [40]. Thus, the model is enhanced and made simpler by the process of removing unnecessary terminology, giving the *Eq. 3*:

$$Y = 142.34 - 39.85\,A + 13.46\,B + 13.31\,D + 25.24\,AB + 7.62\,AD + 23.41\,A^2 \quad (Eq.\ 3)$$

Thus, all previously acquired values by the general empirical model have been amended due to the reduced model adjustment, including the residuals and the predicted values for each experimental combination of process variables. Figure 2 (A2) demonstrates a uniform distribution of the residual for the predicted RPS concentration. The RPS concentration predicted that the plotted *vs* experimental data fit the regression well, with a coefficient of determination (R^2) of 0.9178. The ANOVA statistics results for the reduced model (Table A4) showed a decrease in the model sum of squares and degree of freedom, which is normal, due to the removal of some factors from the model. The fitting adequacy of the model is verified by the model's F-value (92.48), which is far greater than the critical value ($F_{(0.05,6,70)}$=2.215), and the model's *p*-value, which is smaller than 0.0001. The reduced empirical model shows a lower F-value for the residual lack of fits, 1.86, compared to the original value of 1.97, demonstrating an improvement in the model prediction [29]. Furthermore, the R^2 declines (0.8880), but the predicted R^2 (0.8629) and the adjusted R^2 (0.8784) are in good agreement (Table A3), indicating that the model has acceptable parameters.

3.1.2 The effect of process variables on RPS concentration

The reduced empirical model, described by *Eq. 2*, demonstrated that the ratio (cyanobacterial biomass/culture medium) (A), days (B) and nitrogen concentration (D) have a positive effect on the RPS production. The same is not true for the phosphorous concentration (C), which has been shown not to significantly impact RPS production. Figure 3 demonstrates the impact of the ratio and days on the RPS concentration, with the model parameters C=1.25 ([P]) and D=6.25 ([N]) on the centre level in the form of the predicted response of the process in a three-dimensional (3D) plot of the response surface. Centre points present themselves as fixed values set halfway between the low and high settings of the factor. It is possible to verify that an increase in the ratio causes a decrease in the RPS production on day 1, decreasing from 213.9 mg/dm^3 (Day 1 – Ratio 1) to 90.0 mg/dm^3 (Day 1- Ratio 14). During the experimental time, an increased RPS production in the higher ratios is verified, jumping from 90.0 mg/dm^3 (Day 1) to 160.789 mg/dm^3 (Day 7). The same doesn't occur in the lower ratios, where the RPS concentration decreases from 213.9 mg/dm^3 (Day 1) to 190.8 mg/dm^3 (Day 7). With a higher ratio, the cyanobacteria had a higher nutrient concentration, allowing them to develop and produce more RPS. The opposite reaction occurred in the samples with lower ratios, since there is a lack of availability of nutrients; in this situation, the cyanobacteria produce only the necessary components to survive.

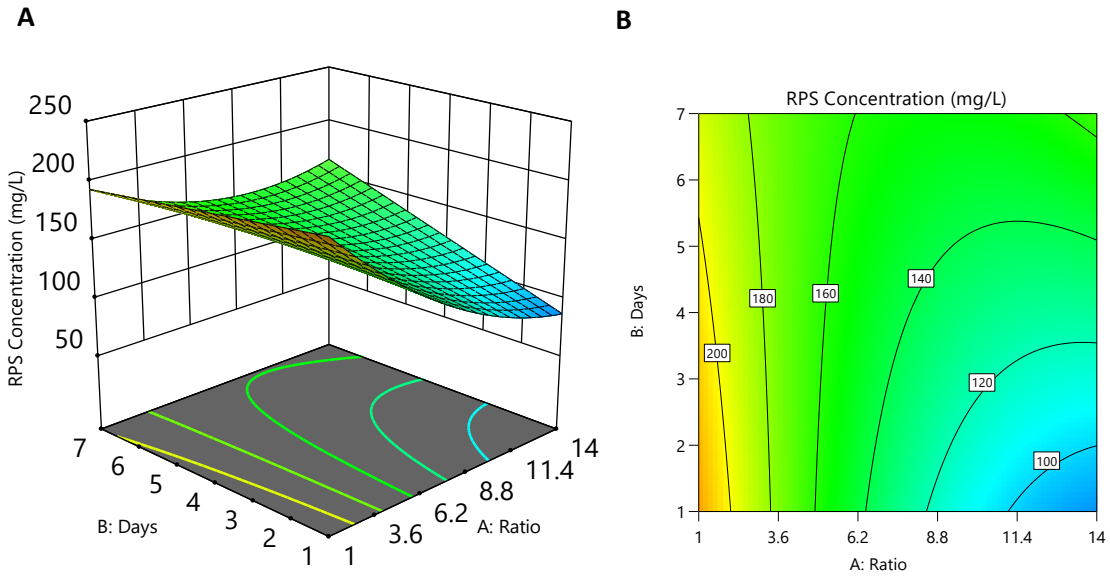

Figure 3 3D Response surface plot representing the response of the process, together with the effects of A (Ratio) and B (Days) on the RPS production **(A)**, and the model parameters C=1.25 ([P]) and D=6.25 ([N]) on the centre level as fixed values **(B)**.

The same behaviour can be seen in Figure 4, demonstrating a decrease in RPS production with the increase in ratio level. These graphs also show the effect of the nitrogen concentration in the culture medium, where a higher concentration contributes to the rise in RPS concentration - 196 mg/dm^3 (A-1/D-2.5) to 207 mg/dm^3 (A-1/D-10) and 105 mg/dm^3 (A-14/D-2.5) to 145 mg/dm^3 (A-14/D-10).

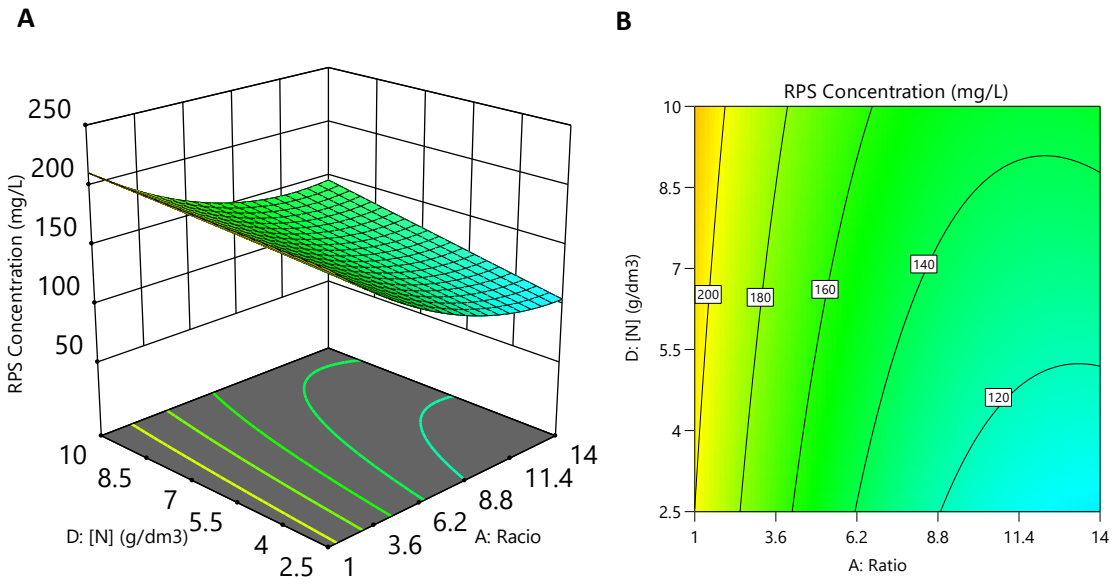

Figure 4 3D Response surface plot representing the response of the process, together with the effects of A (Ratio) and D ([N]) on the RPS production **(A)**, and the model parameters B=4 (Days) and C=1.25 ([P]) on the centre level as fixed values **(B)**.

3.1.3. Method Validation

Significant models with insignificant lack-of-fits present as appropriate tools for predicting and optimising industrial processes. However, method validation is required to verify the predicted responses' veracity. To do so, twenty-six further experiments were conducted using various degrees of independent variables to validate the model that forecasts the RPS concentration after applying the different stress conditions. Factor C (Phosphorus concentration) was left unchanged and kept at the lowest level once it had no discernible impact on the outcome. Table A5 contains the test results and the experimental and predicted responses.

For each of the twenty-six tests, a link between the RPS concentration predicted by the model, and the corresponding value discovered experimentally, is shown in Figure 5. With a

coefficient of determination (R^2) of 0.9206, the findings clearly show that it is possible to validate the model generated. The real experimental values are in agreement with the predicted values.

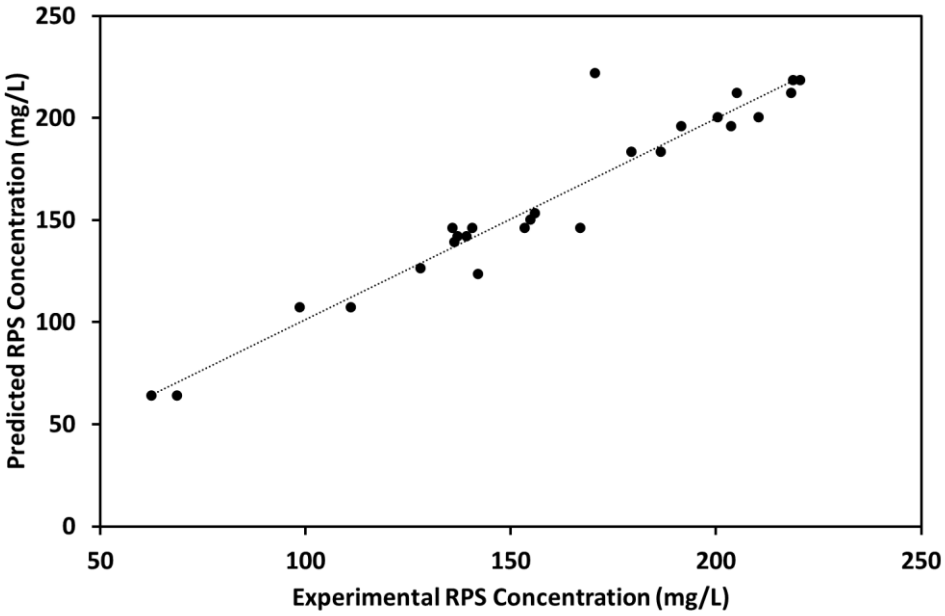

Figure 5 Relationship between the experimental and model predicted RPS production.

In conclusion, using the numerical option of the optimisation module of the design expert program, the levels for each factor were optimised while taking the target value of RPS production (highest possible) into consideration. **It took 1g biomass/6.87mL culture medium for variable A (Ratio), 7 for variable B (Days), 0.98 g/dm^3 for variable C (Phosphorous concentration), and 10 g/dm^3 for variable D (Nitrogen concentration) to achieve the best process for RPS production: a concentration of 113.2 mg/dm^3.** It should be noted that in the optimisation module, the ratio factor was set to be the lowest possible to reduce production costs since the intention is to obtain an industrial-friendly production process.

3.2 Effect of the microplastic contaminated waters in the production of RPS

in an industrial setting, the lower the manufacturing costs of any product, the better. The most economical method to produce RPS for industrial valorisation was from the culture of marine cyanobacteria using seawater. However, it is very likely that the collected saltwater now contains microplastics due to the projected 4900 million tons of plastic debris accumulated in the environment [20]. Therefore, research on the effect of PS-MPs presence should be done to determine how it affects RPS production.

The objective of the present study is to evaluate the *C. cf. calida* -based RPS production behaviour when exposed to PS-MPs, considering the pollution of environmental waters. To study the impact of the RPS production in PS-MPs-contaminated waters, the cyanobacteria under study was treated in various conditions of aeration (static or aerated), PS-MPs concentrations (low (0.05mg/dm^3) and high (5mg/dm^3)), and the cyanobacteria's growth phase (exponential or stationary). Viscosity, biomass and RPS concentration were analysed as indicators of disruption.

Since *C. cf. calida* excretes RPS to the supernatant in response to environmental factors, the viscosity of the supernatant was analysed to track the concentration of RPS using a programmable Rheometer (Brookfield DV-III Ultra Programmable Rheometer) with a spindle 02 at 100 rpm.

3.2.1. RPS production

The experiment started by studying the effect of low (0.05 mg/dm^3) and high (5 mg/dm^3) concentrations of PS-MPs-contaminated waters (Figure 6) on the RPS production by *C. cf. calida*. Statistical treatment was carried out, evaluating the standard deviation of triplicate samples (Table A6). Overall, the statistical treatment showed that all factors (PS-MPs concentration, aeration, growth stage, and days) positively influenced RPS production when subjected individually.

Comparing the initial (Day 1) and final (Day 6) days, RPS concentrations produced under different growth conditions at low and high PS-MPs contamination (Figure 6), the exposition to water contaminated with high PS-MPs concentrations produced higher RPS amounts except for the samples that underwent aeration and were in the exponential growth phase. Thus, using PS-MPs-contaminated waters causes a defensive reaction by *C. cf. calida*, leading to an increase in the RPS concentration.

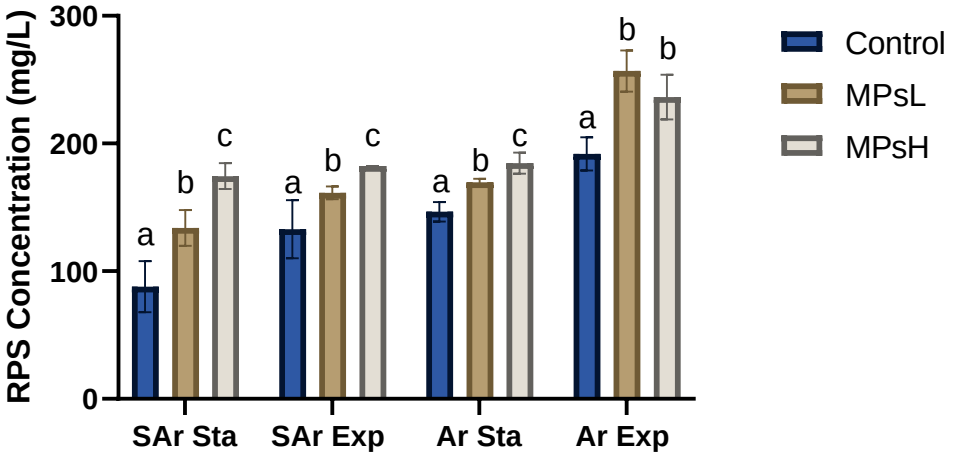

Figure 6 RPS concentration (mg/dm^3) produced under different growth conditions, at low (PS-MPsL) and high MPs contamination (PS-MPsH). Ar- samples submitted to aerated conditions; SAr- samples submitted to static conditions; Sta- samples in the stationary growth phase; Exp- samples in the exponential growth phase. Different letters represent significantly different means of the correspondent RPS concentration for the different growth conditions (*p*-value < 0.05).

Higher PS-MPs contaminated water was used to study the interaction between aeration, growth stage, and days of production.

Analysing Figure 7, it is possible to verify, and as demonstrated by the statistical treatment (Table A6), that the interaction between aeration and growth stage (factors B and C; Table A6) doesn't lead to a significant difference in the viscosity levels over the experimental time, except for the samples collected on day 4, that were not submitted to aeration.

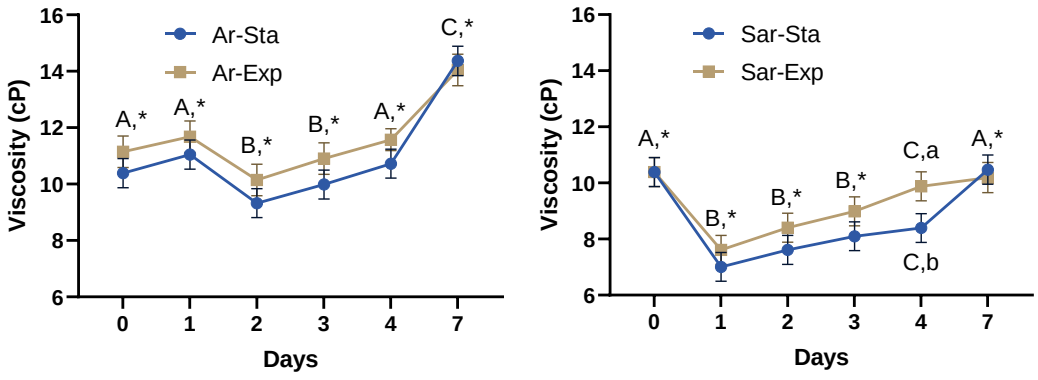

Figure 7 Viscosity along the experimental period in water contaminated with a high concentration of PS-MPs (5 mg/dm^3). Ar- samples submitted to aerated conditions; SAr- samples submitted to static conditions; Sta- samples in the stationary growth phase; Exp- samples in the exponential growth phase. Different letters represent significantly different means of the correspondent day (Capital letters) and significant differences between growth stages (small letters) (*p*-value < 0.05); * represents no significant differences between growth stages (*p*-value ≥ 0.05).

Regarding the variation of viscosity levels over the experimental period, it is possible to verify that samples submitted to aerated conditions showed a decrease in viscosity levels right on day two, followed by an exponential increase. The reduction of the viscosity level on the samples not submitted to aeration is shown sooner on day one, followed by the exponential release of RPS. In general, confirming that higher viscosity values in the samples subjected to aeration is feasible. The highest value recorded for samples subjected to aeration was 14.3 cP (Day 7 Ar-Sta), and the lowest was 9.3 cP (Day 2 Ar-Sta), representing a significant difference from the maximum value of 10.5 cP displayed by the samples under static conditions (Day 7 Sar-Sta).

Regarding the impact of the individual factors on the viscosity result, Figure 8 summarises the effects of the growth stage (factor C) and aeration (factor B) on the viscosity outcome throughout the experimental period (factors D; Table A6). Overall exponential growth phase conditions showed to cause a higher viscosity level, except for the samples collected on day one and the last experimental day. On the other hand, verifying higher viscosity levels on all aerated samples is possible.

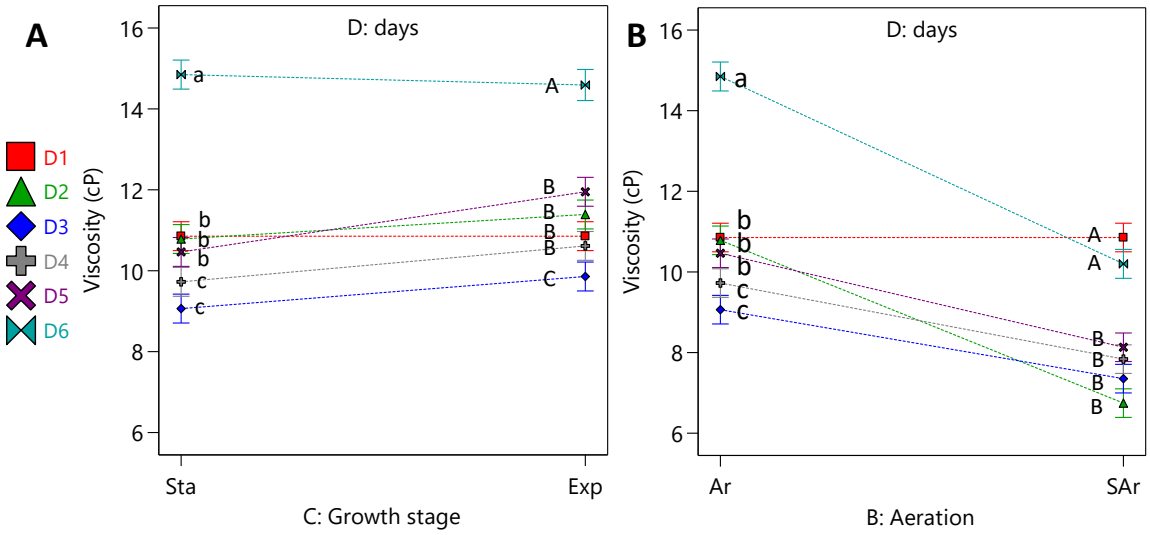

Figure 8 Comparison of viscosity values between stationary and exponential growth **(A)**; Comparison of Viscosity values between aerated and non-aerated samples **(B)**.

3.2.2. Biomass

To understand whether exposure to PS-MPs-contaminated water negatively affects biomass production, with consequent impacts in industrial terms, biomass yield was studied using the same experimental design discussed above (section 3.2.1).

As for RPS production, the comparison of the two-growth phases' impact on biomass production (Figure 9, Table A7) showed not to be statistically significant. However, on day 7 of the samples submitted to aeration, it's possible to verify a significant difference between the two-growth phases.

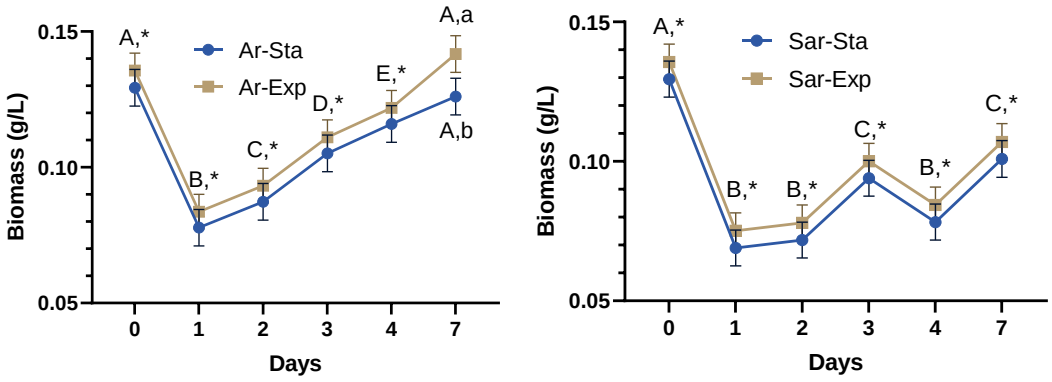

Figure 9 Biomass data along the experimental period (Ar- samples submitted to aeration conditions; Sar- samples submitted to static conditions; Sta- samples in the stationary growth phase; Exp- samples in the exponential growth phase). Different letters represent significantly different means of the correspondent day (Capital letters) and significant differences between

growth stages (small letters) (p-value < 0.05); * represents no significant differences between growth stages (p-value ≥ 0.05)

It is possible to verify a decrease in biomass on day one, independently of the aeration and growth conditions, followed by a significant increase in biomass over the experimental period. Samples that underwent aeration showed an exponential increase in biomass compared to those under static conditions indicating a variation in biomass values. This observation may result from the necessity of aeration conditions for raising alkalinity and, therefore, promoting biomass growth [3].

Figure 10 analysis shows a higher biomass production under aeration conditions, and in the exponential growth phase, except on day one. Biomass and viscosity data are in agreement, suggesting the microalgae's adaptation to microplastic environments. When the PS-MPs solution was first introduced into the cyanobacteria's environment, the first loss in biomass and viscosity may be justified due to necrotic events [20,22]. However, the subsequent increase in biomass and viscosity values shows the cyanobacteria's ability to adapt to any environment.

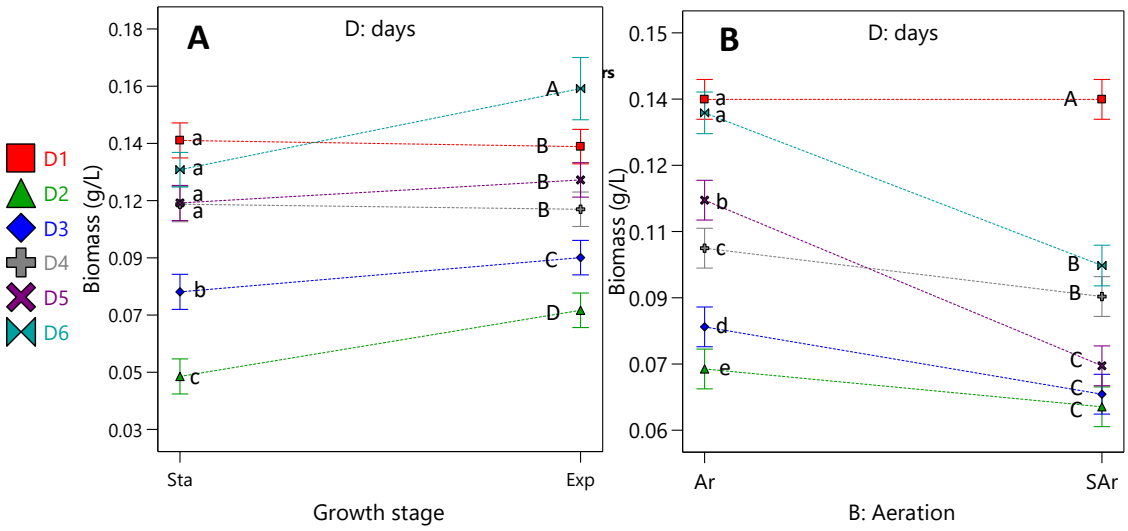

Figure 10 Comparison of biomass values between: stationary and exponential growth **(A)**; aerated and non-aerated samples **(B)**.

In conclusion, when *C. cf. calida* is exposed to PS-MPs-contaminated waters, a defensive reaction occurs proportionally to the PS-MPs concentration. *C. cf. calida* exhibits no issues growing in these; contrarily, it appears that the presence of PS-MPs acts as a stimulator,

increasing RPS and biomass production. It is feasible to confirm the importance of aeration conditions for biomass and RPS production during the exponential growth phase, which showed the maximum value for both biomass and RPS production.

3.3. *C. cf. calida* -based RPS application: bioflocculant agent

During the previously experimental process, and to verify the response of *C. cf. calida* to PS-MPs-contaminated waters, some observations by fluorescent imaging were performed on the cyanobacterial medium (Figure 11 A, A1). The observed retention of PS-MPs in the RPS network demonstrated the potential of the RPS produced by *C. cf. calida* as bioflocculating agents, helpful for treating urban waters. Based on that, the *C. cf. calida* -based RPS were isolated, characterised and studied its flocculant ability.

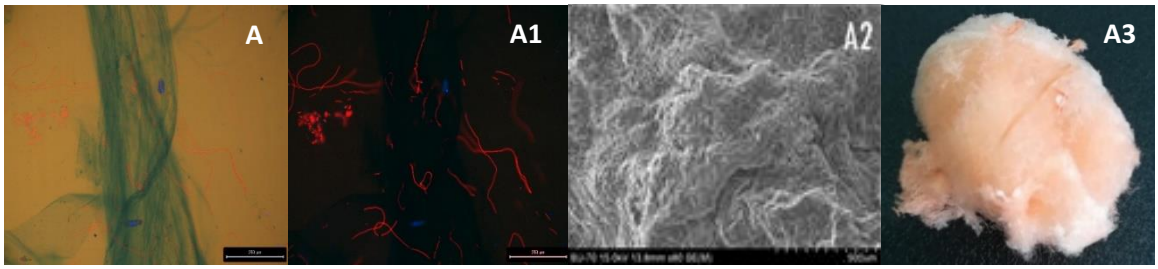

Figure 11 Fluorescence microscopy observation of PS-MPs particles retained in *C. cf. calida* RPS's network stained with Alcian Blue. (10x magnification) **(A, A1)**. Scanning electron microscopy **(A2)**. RPS extracted from *C. cf. calida* culture under aeration **(A3)**.

The *C. cf. calida*-based RPS were isolated from the culture medium by centrifugation and purified using an ultrafiltration technique to remove suspended particles and high-molecular-weight solutes, with a total of 12 consecutive cycles of concentration and dilution (2.5x) with bidistilled water, reaching a constant conductivity (2.7 µS/cm^3; Consort C5020). The ultrafiltration caused a reduction in the viscosity levels of 16 to 21% (Figure A3). This reduction may be due to the ions or low molecular weight sugars and organic acids responsible for the cross-linking of the RPS chains or the alteration of the overall RPS structure [41,42].

In Figure 11 A3, it is possible to visualise the macro appearance of the collected, ultrafiltered and lyophilised RPS. The FTIR (Figure 12) shows a broad band at 3450 cm^{-1}, which is associated with the O-H bond in the hydroxyl groups of carbohydrates. The spectrum also exhibits bands around 2950 cm^{-1}, indicative of the symmetrical and asymmetric stretching of the C-H bonds in the aliphatic CH_2 and CH_3 groups, as well as absorption at a 1420 cm-1 wavelength indicating the deformation of these same groups. The band corresponding to the stretching of the C-O bonds is seen at 1050 cm^{-1} as the band of the stretching of the C=O bond of the carboxyl groups at 1650 cm^{-1} [43,44]. These results unequivocally show the polysaccharide nature of the *C. cf. calida* - based RPS isolated [31,45].

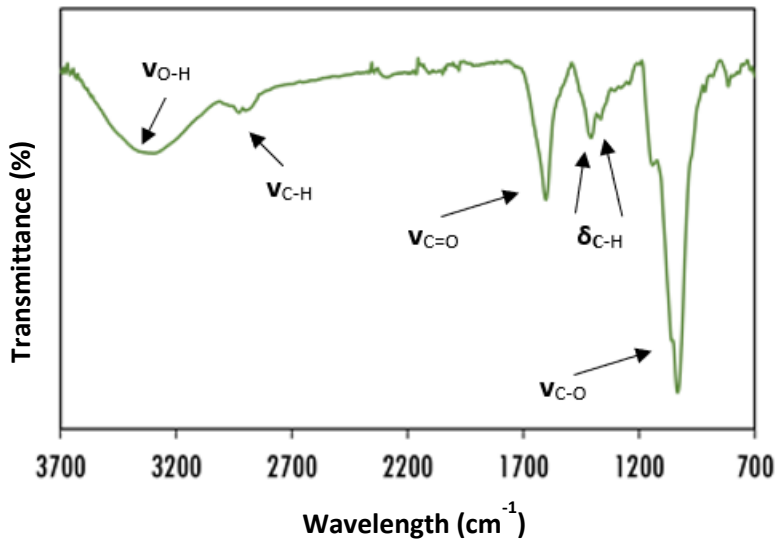

Figure 12 FTIR spectrum of *C. cf. calida* -based RPS isolated and purified by ultrafiltration.

To understand the interactions between the RPS network and PS-MPs, it is crucial to ascertain if the produced RPS have the ability to interact with other particles. For that purpose, the Zeta potential was used to calculate the charge of the biosynthesised RPS and the MPs particles with which they will interact. Zeta potential exhibits the degree of electrostatic attraction, repulsion, or charges between particles [46]. A high zeta potential value (>30 mV) represents an enhanced rate of particle movement under a given electrical field, which inhibits particle sedimentation. On the other hand, at lower zeta potential values, electrostatic repulsion is minimised, and Van der Waals forces facilitate agglomeration [46]. Thus, based on the information provided by the Zeta potential, it is feasible to confirm that PS-MPs and RPS tend to agglomerate since PS-MPs have a Zeta potential of -7.34 ± 0.38 mV and the RPS has -15.50 ± 0.89 mV, both lower than 30mV.

Based on the characterisation of the flocculating agent and to confirm the applicability of RPS for the removal of PS-MPs from highly (2 g/dm^3) contaminated waters with different physico-chemical characteristics, the effects of several parameters, including cation type, cation concentration, pH, salinity, and RPS/MPs ratio, were evaluated.

3.3.1. Cation Effect

As seen in the zeta potential analysis, the PS-MPs under research have a negative charge on their surface. Therefore, positively charged cations will be required to stabilise them. Given

that the RPS have a negative charge on their surface, stabilising the PS-MPs with the addition of cation results in the formation of clusters, meeting our goal of encouraging bioflocculation between the PS-MPs and the RPS (Figure 13).

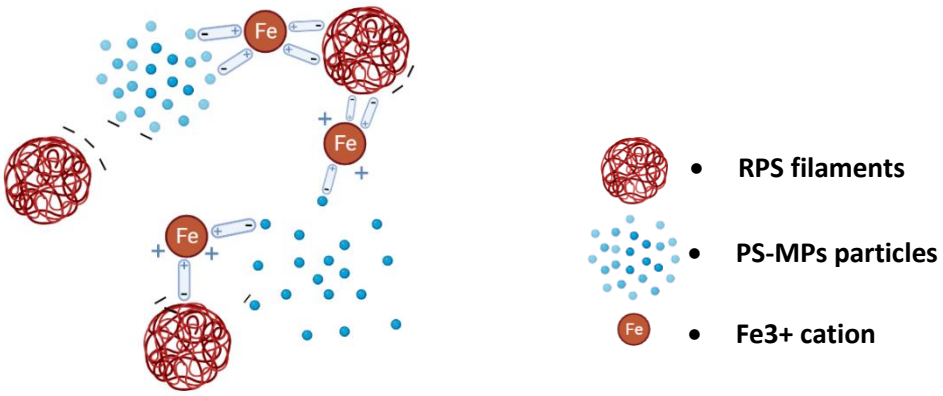

Figure 13 Bioflocculation MPs/Fe^{3+}/RPS process illustration.

By reducing the negative charge of the particle and the polymer, cations can improve the initial absorption of polymers over suspended particles [47]. Using monovalent, divalent, or trivalent cations may affect bioflocculation rates because these cations interact with the negative charges of both the RPS and the suspended particles [48].

Figure 14 (A) resumes the variations in the bioflocculation effect using various cations, namely K^+, Ca^{2+}, Mg^{2+} and Fe^{3+}. Given that PS-MPs have a Zeta potential of -31.2 mV, the cation with the largest charge will provide the greatest electrostatic forces, increasing the agglomeration of PS-MPs particles and, consequently, the bioflocculation rate. As can be seen, aggregates did not develop when the K^+ and Ca^{2+} cation was used. When Fe^{3+} was used, their formation could be seen and gave rise to the significantly highest rate of bioflocculation (82%) for the different types of cation used.

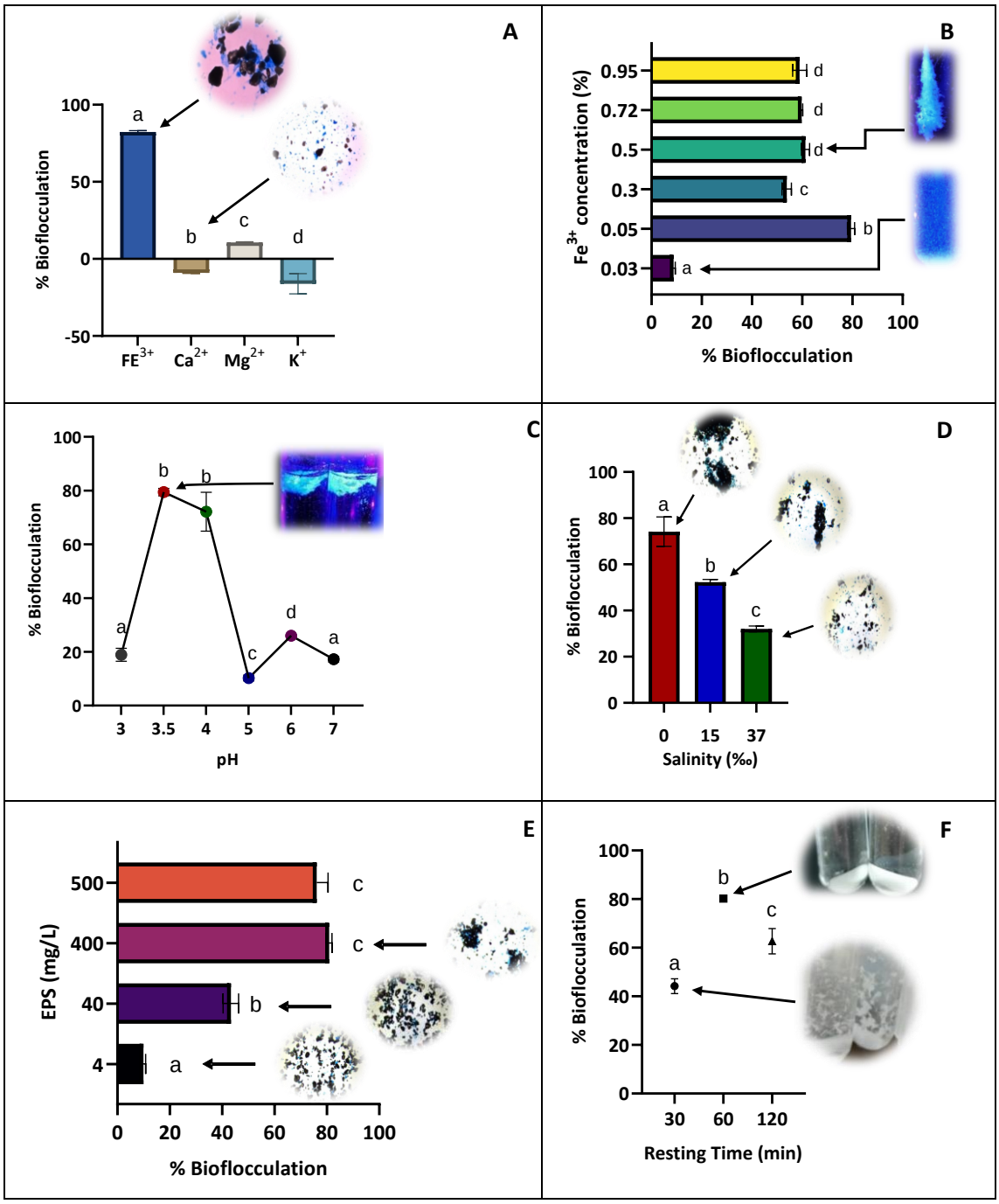

Figure 14 RPS bioflocculation rates obtained for the different types of cations under study. Conditions: 2 g/dm^3 PS-MPs solution, 400 mg/dm^3 RPS solution, cations at 0.448 mM, 0‰ salinity, 60 min rest time and temperature of 25 ± 2°C. Brightfield fluorescence micrographs (5x) of flocculated aggregates composed of *C. cf. calida* -based RPS and PS-MPs (< 100 µm) in the presence of 0.448 mM of Ca^{2+} and Fe^{3+}. **(A)** RPS bioflocculation rates obtained for the different Fe^{3+} concentrations. MPs/Fe^{3+}/RPS aggregates under LED light. Assay using 0.03% Fe^{3+}; Assay using 0.72% Fe^{3+}. **(B)** RPS bioflocculation rates obtained for the different pH under study. MPs/Fe^{3+}/RPS aggregates under LED light pH 3.5. **(C)** RPS bioflocculation rates obtained for the

different salinity levels. Brightfield fluorescence micrographs (5x) of flocculated aggregates composed of *C. cf. calida* RPS and PS-MPs with 0‰, 15‰ and 37‰ salinity. **(D)** RPS bioflocculation rates obtained for the different RPS/MPs ratios. Brightfield fluorescence micrographs (5x) of flocculated aggregates composed of PS-MPs in the presence of (A) 4mg/dm^3, (B) 40 mg/dm^3 and (C) 400mg/dm^3 *C. cf. calida* RPS. **(E)** RPS bioflocculation rates over elapsed time. PS-MPs /Fe^{3+}/RPS aggregates 30 min resting time and 60min resting time. **(F)** Conditions: 2g/dm^3 PS-MPs solution, 400mg/dm^3 RPS solution, 0.05% Fe^{3+} cation, pH 3.5 ± 0.1, 0‰ salinity and temperature of 25 ± 2°C.

In general, cation concentration significantly impacts the bioflocculation process, demonstrating different reactions depending on the type of cation [50]. As a result, the aggregates tended to disperse in the water column or to stay on the surface, depending on the cation concentration.

Since it had the highest bioflocculation efficiency, Fe^{3+} was utilised to assess the effect of cation concentration on bioflocculation rate (Figure 14 B). Fe^{3+} concentration of 0.05% was shown to be the best concentration with higher bioflocculation rates. This seems to suggest that there will be a better charge balance between cations, PS-MPs and RPS at this concentration.

3.3.2. pH Effect

Published works like H. Hadiyanto et al. [51] showed that the impact of pH on flocculation efficiency is quite significant and considerable when it comes to the bioflocculation of microalgae and that flocculation efficiency grows as pH rises.

C. cf. calida -based RPS bioflocculation behaviour is not similar. As reported previously. Among the tested pH, bioflocculation activity is noticeably stronger when exposed to a pH of 3.5 and 4 (rates of 82.31% and 72.16%, respectively). The other pH measurements reveal 46% lower rates (Figure 14C). pH showed a major impact on the bioflocculation procedure.

3.3.3. Salinity Effect

With the objective of knowing the applicability of the RPS in water treatments with different salinities, the rates of bioflocculation of the RPS were determined. It was discovered that in the three salinities evaluated, fresh water (0‰), brackish water (15‰) and salt water (37‰), the rate of bioflocculation was significantly higher (74%) at 0‰ (Figure 14 D). As previously observed, monovalent cation showed much lower bioflocculation values than Fe^{3+},

which can be justified by the increase in the solution's ionic strength, creating competition between Fe^{3+} and Na^{+} ions for PS-MPs. Another possible explanation is the $FeCl_3$ formation, which decreases the interactions between the trivalent cation and the RPS in the solution [52,53]. Furthermore, it is important to note that the size of biopolymers varies with salinity, shrinking as salinity increases with the exception of RPS produced by saltwater microorganisms [54]. These results were confirmed by fluorescence microscopy (Figure 14 D), which shows that the bioflocculation varies within several salinity conditions. According to the micrographs, aggregate formation appears to decrease with salinity increase.

3.3.4. Effect Ratio RPS/ PS-MPs

To minimise costs and maximise flocculation rates, three different ratio RPS/PS-MPs were studied (1/500, 1/50 and 1/5). In order to study the bioflocculation effect of these ratios in water contaminated with PS-MPs (2 g/dm^3), three RPS solutions were prepared (4, 40 and 400 mg/dm^3). When compared to the other concentrations under examination (40 and 4 mg/dm^3), the 400 mg/dm^3 RPS concentration was found to have a significantly higher rate of bioflocculation (Figure 14E). The remnant's greatest rate of bioflocculation indicated a difference of 38% from the highest value (82.31%), showing that greater bioflocculation results from the presence of more amount of RPS. When there is a higher concentration of RPS, a greater agglomeration of PS-MPs is seen. This correlation is directly related to the very high concentrations of PS-MPs (2g/dm^3) used in this study. Thus, and given the ratio of 5MPs/1RPS, *C. cf. calida* -based RPS shows a high flocculation power.

3.3.5. Rest time effect

An essential component of the bioflocculation process is the rest period, where the PS-MPs and RPS interact and for the residual suspended particles in the water column to sediment. The biofloculation rates between the intervals of 30, 60 and 90 minutes were examined. Figure 14F demonstrates the effect of the different resting times in the biofloculation process, showing the highest rate at 60 min (80%). This test indicates that particle aggregation takes time, and in this case, a resting time of 60 minutes produced the greatest bioflocculation results. Contrasting a sample with no resting time and a sample with a resting period of 60 minutes, it is feasible to confirm the impact of this variable - in the sample with no resting time, the flocculate remained suspended, but after a 60-minute rest period, the flocculate sediment.

In conclusion, the purpose of the current study was to investigate the feasibility and efficacy of PS-MPs bioflocculation, with *C. cf. calida* -based RPS, by evaluating the effects of several factors, including PS-MPs size, cation type, cation concentration, pH, salinity, and

RPS/PS-MPs ratio. With a maximum bioflocculation rate of 82%, flocculation was carried out in the presence of trivalent cation Fe^{3+} at 0.05%, pH 3.5 and 25 ± 2 °C. Therefore, it has been demonstrated that *C. cf. calida* RPS are effective bioflocculant agents for the removal of PS-MPs. Thus, the RPS derived from *C. cf. calida* may be a viable and efficient option for the treatment of water contaminated by PS-MPs.

Chapter 4

Conclusions and Perspectives

EPS, or in this case RPS, present a wide range of physicochemical properties that offer them the adaptability to be used in critical commercial and industrial sectors; thus, it is necessary to develop optimum manufacturing processes.

In the present work, three objectives were accomplished: *(i)* propose an industrial operation strategy to enhance RPS production using RSM methodology; *(ii)* evaluate the cyanobacteria behaviour in the presence of PS-MPs; *(iii)* and verify the bioflocculant potential in view of its industrial valorisation, more specifically in wastewater treatment.

Using the RSM, it was possible to optimise the RPS production process. With a ratio of 1/6.87 (*C. cf. calida* biomass/culture medium volume), for 7 days, exposed to a concentration of 0.98 g/dm^3 phosphorous and 10 g/dm^3 of nitrogen concentrations, the best process was achieved - producing 113mg/dm^3 of RPS.

Regarding the behaviour of *C. cf. calida* in the presence of PS-MPs, it was possible to verify that when exposed to water contaminated with higher PS-MPs concentrations, *C. cf. calida* develops a defensive reaction, which results in a higher RPS production. Also, a higher value for both biomass and viscosity was obtained in the exponential growth phase and under aerated conditions.

Finally, it has been shown that *C. cf. calid*-based RPS are efficient bioflocculant agents for PS-MPs removal in highly contaminated waters (2 g/dm^3). To a ratio RPS/PS-MPs of 400 mg/dm^3, a maximum bioflocculation rate of 82% was obtained when flocculation was carried out in the presence of trivalent cation Fe^{3+} at 0.05%, pH 3.5 at 25 ± 2 °C.

References

1- Montoya-Arroyo A., Lehnert K, Lux P, Jimenez V. M., Esquivel P., Silva-Benavides A., Vetter W, Frank J., 2022. 11'-α-Tocomonoenol is the major α-tocomonoenol isomer in cyanobacteria and microalgae from Costa Rica. Journal of Food Composition and Analysis 107, 1-9. https://doi.org/10.1016/j.jfca.2021.104325

2- Singh J.S., Kumar A., Rai A.N. and Singh D.P., 2016. Cyanobacteria: A Precious Bio-resource in Agriculture, Ecosystem, and Environmental Sustainability. Frontiers in Microbiology 7:529. doi: 10.3389/fmicb.2016.00529

3- Asghari S.,Zeinalzadeh K., Kheirfam H., Azar B. H., 2022. The impact of cyanobacteria inoculation on soil hydraulic properties at the lab-scale experiment. Agricultural Water Management 272, 1-10. https://doi.org/10.1016/j.agwat.2022.107865

4- Souza P.O., Sinhor V., Crizel M.G., Pires N., Filho P. S. S., Picoloto R. S., DuarteF. A., Pereira C. M.P., Mesko M. F., 2022. Bioremediation of chromium and lead in wastewater from chemistry laboratories promotes by cyanobacteria. Bioresource Technology Reports 19, 1-6. https://doi.org/10.1016/j.biteb.2022.101161

5- Kastovsky J., Gomez E. B., Hladil J., Johansen J. R., 2014. *Cyanocohniella calida* gen. et sp. nov. (Cyanobacteria: Aphanizomenonaceae) a new cyanobacterium from the thermal springs from Karlovy Vary, Czech Republic. Phytotaxa 181, 279-292. http://dx.doi.org/10.11646/phytotaxa.181.5.3

6- Pereira S., Sousa A., Santos M., Araújo M., Serôdio F., Granja P., Tamagnini P., 2019. Strategies to Obtain Designer Polymers Based on Cyanobacterial Extracellular Polymeric Substances (EPS). International Journal of Molecular Sciences 20, 1-18. doi:10.3390/ijms20225693

7- Klock J. H., Wieland A., Seifert R., Michaelis W., 2007. Extracellular polymeric substances (EPS) from cyanobacterial mats: characterisation and isolation method optimisation. Marine Biology 152, 1077-1085. DOI 10.1007/s00227-007-0754-5

8- Laroche C., 2022. Exopolysaccharides from Microalgae and Cyanobacteria: Diversity of Strains, Production Strategies, and Applications. Marine Drugs 20, 336. https://doi.org/10.3390/md20050336

9- Chug R., Mathur S., Kothari S.L., Harish, Gour V. S., 2021. Maximising EPS production from Pseudomonas aeruginosa and its application in Cr and Ni sequestration. Biochemistry and Biophysics Reports 26 1-6. https://doi.org/10.1016/j.bbrep.2021.100972

10- Liu X., Liu j., Deng D., Li R., Guo C., Ma J., Chen M., 2021. Investigation of extracellular polymeric substances (EPS) in four types of sludge: Factors influencing EPS properties

and sludge granulation. Journal of Water Process Engineering 40, 1-7. https://doi.org/10.1016/j.jwpe.2021.101924

11- Bhattacharyya C., Roy R., Tribedi P., Ghosh A., Ghosh A., 2020. Biofertilisers as substitute to commercial agrochemicals. Agrochemicals Detection, Treatment and Remediation, 263-290. https://doi.org/10.1016/B978-0-08-103017-2.00011-8

12- Cui L., Liu L, Yang Y., Ye S., Luo H., Qiu B., Gao X., 2018. The drnf1 Gene from the Drought-Adapted Cyanobacterium Nostoc flagelliforme Improved Salt Tolerance in Transgenic Synechocystis and Arabidopsis Plant. Genes 9:441. doi:10.3390/genes9090441

13- Phelippe M., Goncalves O., Thouand G., Cogne G., Laroche C., 2019. Characterisation of the polysaccharide's chemical diversity of the cyanobacteria Arthrospira platensis. Algal Research 38, 1-13. https://doi.org/10.1016/j.algal.2019.101426

14- Cruz D., Vasconcelos V., Pierre G., Michaud P., Delattre C, 2020. Exopolysaccharides from Cyanobacteria: Strategies for Bioprocess Development. Applied Sciences 10, 1-20. doi:10.3390/app10113763

15- Abdel-Raouf N., Al-Homaidan A.A., Ibraheem I.B.M., 2012. Microalgae and wastewater treatment. Saudi Journal of Biological Sciences 19, 257-275. http://dx.doi.org/10.1016/j.sjbs.2012.04.005

16- Singh S., Kant C., Yadav R. K., Reddy Y. P., Abraham G., 2019. Cyanobacterial Exopolysaccharides: Composition, Biosynthesis, and Biotechnological Applications. Cyanobacteria, 347-358. https://doi.org/10.1016/B978-0-12-814667-5.00017-9

17- Karpisz K. S., Wiśniewska M.,2018. Flocculation efficiency of the *Sinorhizobium meliloti* 1021 exopolysaccharide relative to mineral oxide suspensions – A preliminary study for wastewater treatment. Separation and Purification Technology 201, 51-59. https://doi.org/10.1016/j.seppur.2018.02.028

18- Iasimone F., Seira J., Quemener E. D., Panico A., Felice V. D, Pirozzi P., Steyer J. P., 2020. Bioflocculation and settling studies of native wastewater filamentous cyanobacteria using different cultivation systems for a low-cost and easy to control harvesting process. Journal of Environmental Management 256, 1-8. https://doi.org/10.1016/j.jenvman.2019.109957

19- Crini G., Lichtfouse E., 2018. Advantages and disadvantages of techniques used for wastewater treatment. Environmental Chemistry Letters 17, 145-155. https://doi.org/10.1007/s10311-018-0785-9

20- Wang R., Zhai M. J. H., Liu Y., 2020. Occurrence of phthalate esters and microplastics in urban secondary effluents, receiving water bodies and reclaimed water treatment

processes. Science of the Total Environment, 1-34. https://doi.org/10.1016/j.scitotenv.2020.140219

21- Treilles R., Gasperi J., Gallard A., Saad M., Dris R., Partibane C., Breton J., Tassin B., 2021. Microplastics and microfibers in urban runoff from a suburban catchment of Greater Paris. Environmental Pollution 287, 1-8. https://doi.org/10.1016/j.envpol.2021.117352

22- Treilles R., Gasperi J., Tramoy R., Dris R., Gallard A., Partibane C., Tassin B., 2022. Microplastic and microfiber fluxes in the Seine River: Flood events versus dry periods. Science of the Total Environment 805, 1-9. https://doi.org/10.1016/j.scitotenv.2021.150123

23- Singh P., Shera S. S., Banik J., Banik R. M. 2013. Optimisation of cultural conditions using response surface methodology versus artificial neural network and modelling of L-glutaminase production by Bacillus cereus MTCC 1305. Biore source Technology 137, 261-269. http://dx.doi.org/10.1016/j.biortech.2013.03.086

24- reig S. J. M., Luti K. J. K., 2021. Response surface methodology: A review on its applications and challenges in microbial cultures. Materials Today: Proceedings 42, 2277-2284. https://doi.org/10.1016/j.matpr.2020.12.316

25- Domagalski N. R., Mack B. C., Tabora J., 2015. On the Analysis of Design of Experiments with Dynamic Responses. Organic Process Research & Development, 1-52. DOI: 10.1021/acs.oprd.5b00143

26- Ramus, J. 1977. Alcian Blue: a quantitative aqueous assay for algal acid and sulfated polysaccharides. J. Phycol. 13. 345-348.

27- MEYERS R. H., MONTGOMERY D. C., COOK C. M. A. Process and Product Optimisation Using Designed Experiments. RESPONSE SURFACE METHODOLOGY 3. Canada. John Wiley & Sons, Inc. 2009

28- amos J., 1977. Alcian Blue: A quantitative aqueous assay for algal acid and sulphated polysaccharides. J. Phycol. 13, 345-348.

29- DOUGLAS C. MONTGOMERY. Design and Analysis of Experiments. Arizona. John Wiley & Sons, Inc. 2013

30- Mutwiri E., Mwenda E., Karanja S., 2015. Effects of Temperature-Dependent Viscosity and Viscous Dissipation on Fluid Flow past a Moving Isothermal Flat Plate. International Journal of Innovative Science, Engineering & Technology 3, 1-12.

31- Mota R., Guimarães R., Büttel Z., Rossi F., Colica G., Silva C. J., Santos C., Gales L., Zille A., Philippis R., Pereira S. B., Tamagnini P., 2013. Production and characterisation of extracellular carbohydrate polymer from *Cyanothece* sp. CCY 0110. Carbohydrate Polymers 92, 1408-1415. https://doi.org/10.1016/j.carbpol.2012.10.070

32- Mathur S., 2013. Extracellular Polymeric Substances from Cyanobacteria: Characteristics. Isolation and Biotechnological Applications-A. *International Journal of Advances in Engineering, Science and Technology (IJAEST)*, 49–53.

33- Solovchenko A., Gorelova O., Karpova O., Selyakh I., Semenova L., Chivkunova O., Baulina O., Vinogradova E., Pugacheva T., Scherbakov P., Vasilieva S., Lukyanov A., Lobakova E., 2020. Phosphorus Feast and Famine in Cyanobacteria: Is Luxury Uptake of the Nutrient Just a Consequence of Acclimation to Its Shortage? Cells 9, 1-22. doi:10.3390/cells9091933

34- Stal, Lucas J, 2015. Nitrogen Fixation in Cyanobacteria. In: eLS. John Wiley & Sons, Ltd: Chichester. DOI: 10.1002/9780470015902.a0021159.

35- Zimmer F. C., Souza A. H. P., Silveira A. F. C., Santos M. R., Matsushita M., SouzaN. E., Rodrigues A. C., 2017. Application of Factorial Design for Optimisation of the Synthesis of Lactulose Obtained from Whey Permeate. Journal of the Brazilian Chemical Society 28, 1-8. DOI:10.21577/0103-5053.20170083

36- CZITROM V., 1999. One-Factor-at-a-Time Versus Designed Experiments. The American Statistician 53, 126-131. https://doi.org/10.1080/00031305.1999.10474445.

37- Maouche N. H., Bacha S. B., Hammache F. O., 2009. Design of experiments for the modelling of the phenol adsorption process, J. Chem. Eng. Data. 54, 2874-2880. https://doi.org/10.1021/je800959k.

38- Anderson-Cook C. M., 2008. Response Surfaces, Mixtures, and Ridge Analyses. Journal of the American Statistical Association 103, 888. https://doi.org/10.1198/jasa.2008.s238

39- Brereton R. G., 2019. The use and misuse of p values and related concepts. Chemometrics and Intelligent Laboratory Systems 195, 1-7. https://doi.org/10.1016/j.chemolab.2019.103884

40- Govaerts B., Francq B., Marion R., Martin M., Thiel M., 2020. The Essentials on Linear Regression, ANOVA, General Linear and Linear Mixed Models for the Chemist. Comprehensive Chemometrics 2, 1-33. https://doi.org/10.1016/b978-0-12-409547-2.14579-2.

41- Tinzl-Malang S. K., Grattepanche F., Rast P., Fischer P., Sych J., Lacroix C., 2020. Purified exopolysaccharides from Weissella confusa 11GU-1 and Propionibacterium freudenreichii JS15 act synergistically on bread structure to prevent staling. LWT - Food Science and Technology 127, 1-8. https://doi.org/10.1016/j.lwt.2020.109375

42- Wear M. P., Hargett A. A., Kelly J. E., McConnell S. A., Crawford C. J., Freedberg D. I., Stark R. E., Casadevall A., 2022. Lyophilization induces physicochemical alterations in

cryptococcal exopolysaccharide. Carbohydrate Polymers 291, 1-9. https://doi.org/10.1016/j.carbpol.2022.119547

43- Bhatnagar M., Parwani L., Sharma V., Ganguly J., Bhatnagar A., 2014. Exopolymers from *Tolypothrix tenuis* and three *Anabaena* sp. (Cyanobacteriaceae) as novel blood clotting agents for wound management. Carbohydrate Polymers 99, 692-699. https://doi.org/10.1016/j.carbpol.2013.09.005

44- Parikh A., Madamwar D., 2006. Partial characterisation of extracellular polysaccharides from cyanobacteria. Bioresource Technology 15, 1822-1827. https://doi.org/10.1016/j.biortech.2005.09.008

45- Pereira S., Zille A., Micheletti E., Ferreira P. M., Philippis R., Tamagnini P., 2009. Complexity of cyanobacterial exopolysaccharides: Composition, structures, inducing factors and putative genes involved in their biosynthesis and assembly. *FEMS Microbiology Reviews*, *33*, 917–941. https://doi.org/10.1111/j.1574-6976.2009.00183.x

46- Hanaor D., Michelazzi M., Leonelli C., Sorrell C. C., 2012. The effects of carboxylic acids on the aqueous dispersion and electrophoretic deposition of ZrO2. *Journal of the European Ceramic Society 32*, 235–244. https://doi.org/10.1016/j.jeurceramsoc.2011.08.015

47- Zhu C., Chen C., Zhao L., Zhang Y., Yang J., Song L., Yang, S., 2012. Bioflocculant produced by Chlamydomonas reinhardtii. *Journal of Applied Phycology 24*, 1245–1251. https://doi.org/10.1007/s10811-011-9769-x

48- Li W. W., Zhou W. Z., Zhang Y. Z., Wang J., Zhu X. B., 2008. Flocculation behaviour and mechanism of an exopolysaccharide from the deep-sea psychrophilic bacterium Pseudoalteromonas sp. SM9913. *Bioresource Technology*, *99*, 6893–6899. https://doi.org/10.1016/j.biortech.2008.01.050

49- Azevedo A. C., Bonumá, A. S., 2004. Colloidal particles, dispersion and aggregation in Latossolos (Oxisols). Ciência Rural 34, 609–617. https://doi.org/10.1590/s0103-84782004000200046

50- Sobeck D. C., Higgins M. J., 2002. Examination of three theories for mechanisms of cation-induced bioflocculation. Water Research 3, 527-538. https://doi.org/10.1016/S0043-1354(01)00254-8

51- Hadiyanto H., Widayat W., Pratiwi M. E., Christwardana M., Muylaert K., 2022. Effect of pH, cationic inducer, and clam shells as bio-flocculant in the optimisation of the flocculation process for enhanced microalgae harvesting using response surface methodology. Environmental Pollutants and Bioavailability 34, 338-351. https://doi.org/10.1080/26395940.2022.2110520

52- Connick R. E., Coppel C. P., 1959. Kinetics of the Formation of the Ferric Chloride Complex. *Angewandte Chemie International Edition 6, 951–952. 81*(1), 6389–6394.

53- Alimi O. S., Farner Budarz J., Hernandez L. M., Tufenkji N., 2018. Microplastics and Nanoplastics in Aquatic Environments: Aggregation, Deposition, and Enhanced Contaminant Transport. In *Environmental Science and Technology.* American Chemical Society 52, 1704–1724. https://doi.org/10.1021/acs.est.7b05559

54- Lam G.P., Giraldo J. B., Vermuë M. H., Olivieri G., Eppink M. H. M., Wijffels R. H., 2016. Understanding the salinity effect on cationic polymers in inducing flocculation of the microalga Neochloris oleoabundans. Journal of Biotechnology 225, 1-8. http://dx.doi.org/10.1016/j.jbiotec.2016.03.009

55- Singh S., Kant C., Yadav R. K., Reddy Y. P., Abraham G., 2019. Cyanobacterial Exopolysaccharides: Composition, Biosynthesis, and Biotechnological Applications. Cyanobacteria, 347-358. https://doi.org/10.1016/B978-0-12-814667-5.00017-9

Appendix

Spirulina medium constitution

macronutrients: 13.61 g.L^{-1} dH_2O $NaHCO_3$; 4.03 g.L^{-1} Na_2CO_3; 0.50 g.L^{-1} K_2HPO_4; 2.5 g.L^{-1} $NaNO_3$; 1.0 g.L^{-1} K_2SO_4; 1.0 g.L^{-1} NaCl; 0.2 g.L^{-1} $MgSO_4.7H_2O$; 0.04 g.L^{-1} $CaCl_2.2H_2O$; 0.08 g.L^{-1} $Na_2EDTa.2H_2O$; micronutrients: 0.8 g.L^{-1} $Na_2EDTA.2H_2O$; 0.7 g.L^{-1} $FeSO_4.7H_2O$; 0.1 g.100ml^{-1} $ZnSO_4.7H_2O$; 0.1 g.100ml^{-1} $MnSO_4.7H_2O$; 0.2 g.100ml^{-1} H_3BO_3; 0.02 g.100ml^{-1} $Co(NO_3)2.6H_2O$; 0.02 g.100ml^{-1} $Na_2MoO_4.2H_2O$; 0.0005 g.100ml^{-1} $CuSO_4.5H_2O$, 1 ml Vitamins (0.000005 g.L^{-1} Vitamin B12)

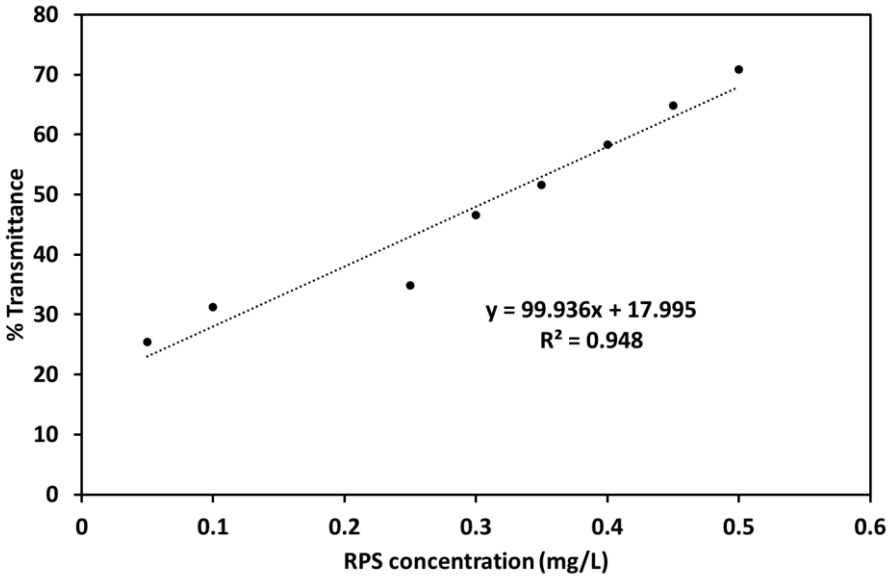

Figure A1 Linear regression determining the relation between concentration of compound (RPS) and transmittance (%) in the spectrophotometer. All determinations were carried out in triplicate.

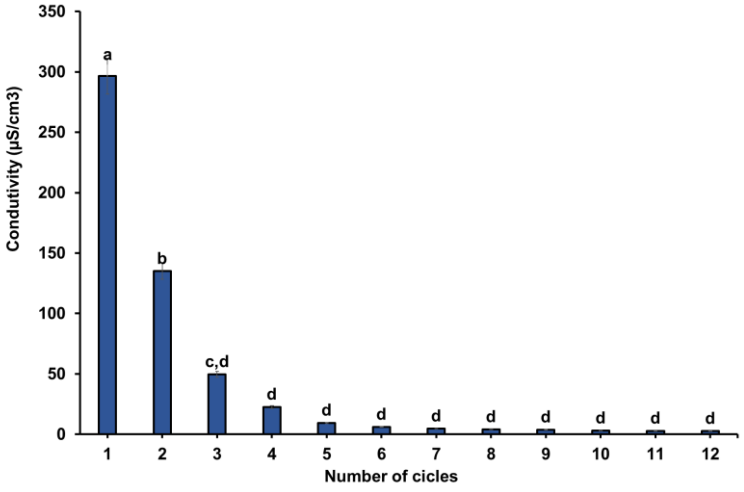

Figure A2 Conductivity curve over the number of ultrafiltration cycles. Different letters represent significantly different means of the correspondent conductivity over the number of cycles (p-value < 0.05).

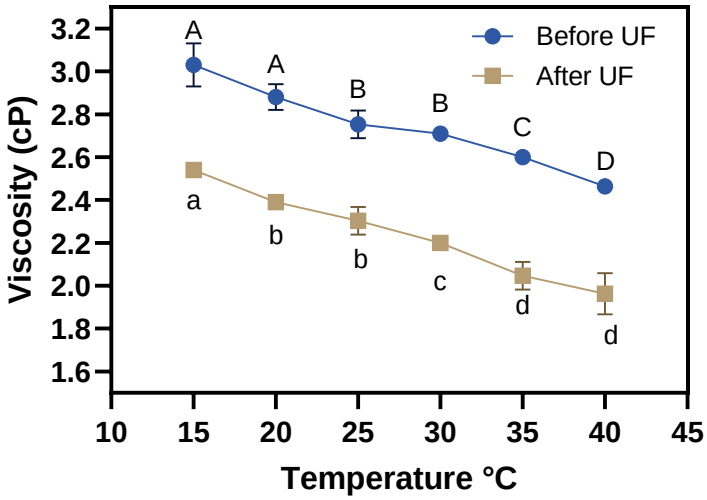

Figure A3 Viscosity levels with different temperatures before and after ultrafiltration. Different letters represent significantly different means of the correspondent viscosity over the temperature spectrum (p-value < 0.05).

Table A1 Three-level and four-factor fractional experimental design and associated response (experimental and predicted RPS Concentration(mg/g)). **A:** Racio; **B:** Days; **C:** Phosphorus concentration; **D:** Nitrogen concentration

Run	Conditions				RPS Concentration (mg/dm^3)	
	A	B	C	D	Experimental	Predicted
1	7.50	4.00	1.25	6.25	169	147
2	7.50	4.00	1.25	6.25	181	147
3	7.50	4.00	1.25	6.25	150	147
4	1.00	1.00	0.50	2.50	193	199
5	7.50	4.00	0.50	6.25	133	135
6	1.00	7.00	2.00	10.00	210	204
7	1.00	7.00	0.50	10.00	190	195
8	14.00	7.00	2.00	10.00	188	171
9	1.00	1.00	0.50	10.00	230	209
10	1.00	7.00	0.50	10.00	192	195
11	1.00	1.00	0.50	2.50	184	199
12	1.00	1.00	2.00	10.00	247	227
13	1.00	1.00	2.00	10.00	219	227
14	14.00	4.00	1.25	6.25	142	144
15	1.00	1.00	2.00	2.50	231	225
16	14.00	4.00	1.25	6.25	128	144
17	1.00	7.00	0.50	2.50	140	187
18	7.50	1.00	1.25	6.25	126	128
19	1.00	7.00	2.00	2.50	213	204
20	7.50	4.00	1.25	2.50	129	131
21	14.00	1.00	2.00	2.50	83	60
22	14.00	1.00	2.00	10.00	92	100
23	7.50	4.00	2.00	6.25	135	137
24	1.00	1.00	0.50	10.00	205	209
25	14.00	7.00	2.00	2.50	135	134
26	7.50	4.00	1.25	6.25	152	147
27	1.00	4.00	1.25	6.25	225	227
28	14.00	7.00	2.00	2.50	125	134
29	7.50	1.00	1.25	6.25	116	128
30	14.00	7.00	2.00	2.50	134	134
31	7.50	4.00	2.00	6.25	127	137
32	14.00	1.00	0.50	2.50	78	67
33	7.50	7.00	1.25	6.25	168	158
34	14.00	1.00	2.00	2.50	68	60
35	14.00	4.00	1.25	6.25	136	144
36	14.00	7.00	0.50	10.00	190	194
37	14.00	1.00	0.50	10.00	113	114
38	7.50	4.00	2.00	6.25	131	137
39	1.00	4.00	1.25	6.25	226	227
40	1.00	7.00	2.00	10.00	206	204
41	14.00	1.00	0.50	2.50	61	67
42	14.00	7.00	0.50	2.50	149	149

Run	Conditions				RPS Concentration (mg/dm^3)	
	A	B	C	D	Experimental	Predicted
43	7.50	4.00	0.50	6.25	131	135
44	1.00	7.00	0.50	2.50	267	187
45	1.00	7.00	2.00	2.50	185	204
46	14.00	7.00	2.00	10.00	172	171
47	1.00	7.00	0.50	2.50	192	187
48	14.00	1.00	2.00	10.00	91	100
49	14.00	7.00	0.50	2.50	148	149
50	1.00	4.00	1.25	6.25	228	227
51	14.00	7.00	2.00	10.00	160	171
52	14.00	1.00	2.00	10.00	97	100
53	1.00	7.00	0.50	10.00	154	195
54	7.50	4.00	1.25	10.00	160	155
55	7.50	4.00	1.25	2.50	113	131
56	7.50	4.00	1.25	6.25	153	147
57	14.00	1.00	0.50	10.00	112	114
58	7.50	7.00	1.25	6.25	158	158
59	7.50	4.00	1.25	10.00	158	155
60	14.00	1.00	2.00	2.50	68	60
61	14.00	1.00	0.50	2.50	72	67
62	14.00	7.00	0.50	2.50	133	149
63	14.00	1.00	0.50	10.00	113	114
64	7.50	1.00	1.25	6.25	105	128
65	7.50	4.00	1.25	2.50	119	131
66	7.50	4.00	1.25	10.00	154	155
67	1.00	1.00	0.50	2.50	202	199
68	1.00	7.00	2.00	2.50	205	204
69	7.50	4.00	1.25	6.25	157	147
70	1.00	1.00	2.00	2.50	223	225
71	1.00	1.00	2.00	2.50	220	225
72	7.50	4.00	0.50	6.25	132	135
73	1.00	1.00	0.50	10.00	219	209
74	1.00	1.00	2.00	10.00	220	227
75	14.00	7.00	0.50	10.00	201	194
76	14.00	7.00	0.50	10.00	212	194
77	1.00	7.00	2.00	10.00	204	204
78	7.50	7.00	1.25	6.25	161	158

Table A2 Analysis of variance (ANOVA) extended model. **A:** Racio; **B:** Days; **C:** Phosphorus concentration; **D:** Nitrogen concentration

Source	Sum of squares	Degree of freedom	Mean Square	F-value	p-value
Model	$1.59x10^5$	14	11361.83	40.06	< 0.0001
A	92171.23	1	92171.23	325.02	< 0.0001
B	12026.63	1	12026.63	42.41	< 0.0001
C	33.53	1	33.53	0.12	0.7321
D	7578.77	1	7578.77	26.72	< 0.0001
AB	26725.88	1	26725.88	94.24	< 0.0001
AC	3082.14	1	3082.14	10.87	0.0016
AD	4119.63	1	4119.63	14.53	0.0003
BC	239.76	1	239.76	0.85	0.3614
BD	10.33	1	10.33	0.04	0.8492
CD	175.79	1	175.79	0.62	0.4340
A^2	11017.20	1	11017.20	38.85	< 0.0001
B^2	141.23	1	141.23	0.50	0.4830
C^2	1029.33	1	1029.33	3.63	0.0613
D^2	153.57	1	153.57	0.54	0.4645
Residual	17865.95	63	283.59		
Lack of Fit	4834.92	10	483.49	1.97	0.0561
Pure Error	13031.03	53	245.87		

Table A3 Coefficient of determination statistics for RPS concentration.

Statistics	Response: RPS Concentration (mg/dm^3)	
	Extended model	Reduced model
Predicted R^2	0.9092	0.8629
Adjusted R^2	0.9285	0.8784
R^2	0.9417	0.8880

Table A4 Analysis of variance (ANOVA) reduced model. **A:** Racio; **B:** Days; **C:** Phosphorus concentration; **D:** Nitrogen concentration

Source	Sum of squares	Degree of freedom	Mean Square	F-value	p-value
Model	$1.467x10^5$	6	24450.32	92.48	< 0.0001
A	83999.52	1	83999.52	317.72	< 0.0001
B	9583.41	1	9583.41	36.25	< 0.0001
D	9370.07	1	9370.07	35.44	< 0.0001
AB	29880.44	1	29880.44	113.02	< 0.0001
AD	2721.69	1	2721.69	10.29	0.0020
A^2	9050.72	1	9050.72	34.23	< 0.0001
Residual	18506.94	70	264.38		
Lack of Fit	3586.34	8	448.29	1.86	0.0823
Pure Error	14920.61	62	240.65		

Table A5 Conditions of validation alongside with the actual and predicted values. **A:** Racio; **B:** Days; **C:** Phosphorus concentration; **D:** Nitrogen concentration

Run	Condition				RPS Concenration (mg/dm^3)	
	A	B	C	D	Actual	Predicted
1	1.00	1.00	0.50	2.50	205	212
2	14.00	1.00	0.50	2.50	62	64
3	1.00	7.00	0.50	2.50	204	196
4	14.00	7.00	0.50	2.50	139	142
5	1.00	1.00	0.50	2.50	218	212
6	14.00	1.00	0.50	2.50	69	64
7	1.00	7.00	0.50	2.50	192	196
8	14.00	7.00	0.50	2.50	137	142
9	1.00	1.00	0.50	10.00	220	219
10	14.00	1.00	0.50	10.00	111	107
11	1.00	7.00	0.50	10.00	200	200
12	14.00	7.00	0.50	10.00	187	183
13	1.00	1.00	0.50	10.00	219	219
14	14.00	1.00	0.50	10.00	99	107
15	1.00	7.00	0.50	10.00	210	200
16	14.00	7.00	0.50	10.00	179	183
17	1.00	4.00	0.50	6.25	170	222
18	14.00	4.00	0.50	6.25	136	139
19	7.50	1.00	0.50	6.25	142	124
20	7.50	7.00	0.50	6.25	156	154
21	7.50	4.00	0.50	6.25	136	146
22	7.50	4.00	0.50	6.25	141	146
23	7.50	4.00	0.50	2.50	128	127
24	7.50	4.00	0.50	10.00	155	150
25	7.50	4.00	0.50	6.25	153	146
26	7.50	4.00	0.50	6.25	167	146

Table A6 Analysis of variance (ANOVA) for the viscosity data. **A:** MPs concentration; **B:** Aeration; **C:** Growth stage; **D:** Days

Source	Sum of squares	Degree of freedom	Mean Square	F-value	p-value
A-[MPs]	2.750	2	1.380	4.2300	0.0180
B-Aeration	191.780	1	191.780	589.3800	< 0.0001
C-Growth stage	14.230	1	14.230	43.7200	< 0.0001
D-Days	214.740	5	42.950	131.9900	< 0.0001
AB	0.790	2	0.395	1.2100	0.3026
AC	3.920	2	1.960	6.0200	0.0037
AD	8.570	10	0.857	2.6300	0.0080
BC	0.004	1	0.004	0.0115	0.9148
BD	78.000	5	15.600	47.9500	< 0.0001
CD	10.310	5	2.060	6.3300	< 0.0001
ABC	2.000	2	1.000	3.0800	0.0516
ABD	15.080	10	1.510	4.6300	< 0.0001
ACD	4.600	10	0.460	1.4100	0.1895
BCD	3.490	5	0.698	2.1400	0.0687

Table A7 Analysis of variance (ANOVA) for the Biomass data. **A:** MPs concentration; **B:** Aeration; **C:** Growth stage; **D:** Days

Source	Sum of squares	Degree of freedom	Mean Square	F-value	p-value
A-[MPs]	0.0008	2	0.0004	10.04	0.0001
B-Aeration	0.0105	1	0.0105	272.20	< 0.0001
C-Growth stage	0.0013	1	0.0013	33.36	< 0.0001
D-days	0.0697	5	0.0139	361.97	< 0.0001
AB	0.0005	2	0.0002	5.91	0.0041
AC	0.0012	2	0.0006	15.72	< 0.0001
AD	0.0022	10	0.0002	5.82	< 0.0001
BC	0.0004	1	0.0004	10.13	0.0021
BD	0.0066	5	0.0013	34.07	< 0.0001
CD	0.0016	5	0.0003	8.29	< 0.0001
ABC	0.0005	2	0.0002	6.22	0.0031
ABD	0.0027	10	0.0003	7.00	< 0.0001
ACD	0.0013	10	0.0001	3.48	0.0008
BCD	0.0018	5	0.0004	9.60	< 0.0001